

Supporting Information

A Chiroptical Approach for the Absolute Stereochemical Determination of P-Stereogenic Center

Debarshi Chakraborty, Hadi Gholami, Aritra Sarkar, Leo A. Joyce, James E. Jackson, and Babak Borhan*

babak@chemistry.msu.edu

Table of Contents:

I.	Materials and General Instrumentations:.....	2
II.	General Procedure for UV-vis Measurements, Binding Affinity Calculations and Jobs Plot Analysis:.....	3
III.	General Procedure for CD Measurement:	6
IV.	Temperature Dependence on the Amplitude of the ECCD Signal for Zn-MAPOL 2 Complexed with R_P -4d	17
V.	Solvent Screen for Zn-MAPOL 2 Complexed with R_P -4d and R_P -4g.	19
VI.	ECCD of MeO-Zn-MAPOL 3 Complexed with Chiral Phosphorous Oxide	22
VII.	Experimental Procedure:.....	24
VIII.	Crystal Structure of R_P -4d bound to Zn-TPP:.....	29
IX.	References:	30
X.	NMR Spectra:	31

I. Materials and General Instrumentations:

Anhydrous solvents used for CD measurements were purchased from Aldrich and were spectra grade. Unless otherwise mentioned, solvents were purified as follows. CH₂Cl₂ was dried over CaH₂ whereas THF and Et₂O were dried over sodium (dryness was monitored by colorization of benzophenone ketyl radical); they were freshly distilled prior to use. NMR spectra were obtained using 500 MHz Varian NMR spectrometers and referenced using the residual ¹H peak from the deuterated solvent for the proton NMR, the carbon shift of the solvent (77.0 ppm for CDCl₃) for the ¹³C-NMR, and phosphoric acid (as the internal standard reference for the ³¹P-NMR measurements. Column chromatography was performed using Silicycle 60 Å, 35-75 μm silica gel. Pre-coated 0.25 mm thick silica gel 60 F254 plates were used for analytical TLC and visualized using UV light, *p*-anisaldehyde stain or phosphomolybdic acid in EtOH stain. CD spectra were recorded on a JASCO J-810 spectropolarimeter, equipped with a temperature controller (Neslab 111) for low temperature studies, and are reported as Mol. CD / λ [nm]. UV-vis spectra were recorded on an Agilent, Cary 100 UV-visible spectrophotometer equipped with temperature controller. UV spectra were collected with scan rate of 100 nm/min. Sofosbuvir and *epi*-sofosbuvir were generously gifted from Merck, Inc.

II. General Procedure for UV-vis Measurements, Binding Affinity Calculations and Jobs Plot Analysis:

UV-vis measurement: Zn-MAPOL **2** (1.0 μL of a 0.001M solution in anhydrous dichloromethane, 1.0 μmol) was added to hexane (1.0 mL) in a 1.0 cm UV-cell. The background spectrum was recorded from 350 nm to 480 nm at a scan rate of 100 nm/min. Chiral phosphorus oxides (1 up to 500 equivalents) from four different stock solutions in anhydrous dichloromethane [0.1M (for 100-500 equiv), 0.01M (for 10-100 equiv), 0.001M (for 1-10 equiv), 0.0001M (for 0.1-1 equiv)] were then added to the Zn-MAPOL **2** solution. The UV spectra were collected after each addition. A representative UV-vis titration graph is shown below (Figure S1).

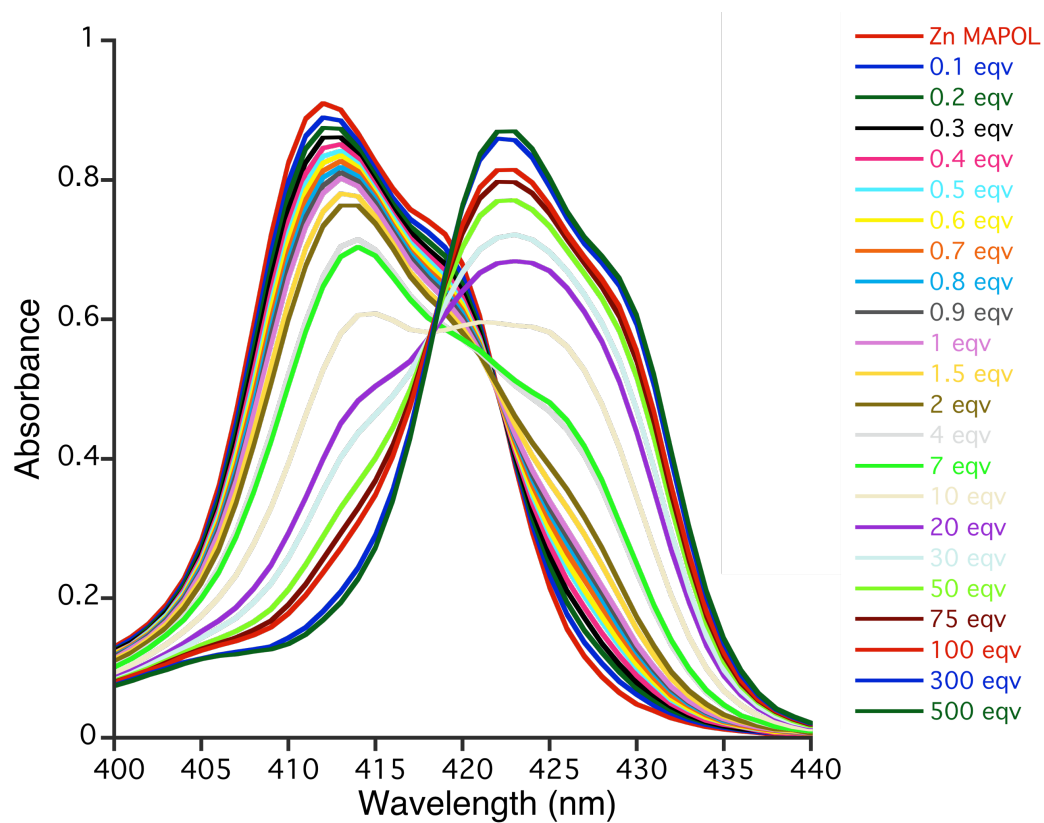


Figure S1. UV-vis titration of Zn-MAPOL 2 (1 μM) with *R_p*-4d at 0 °C in hexane.

Binding affinity measurements: Data gathered from the titration of analytes with Zn-MAPOL **2** were used to obtain binding affinities, as described previously.¹ Figure S2 depicts the binding affinity measured for *R_P-4d* bound to **2**.

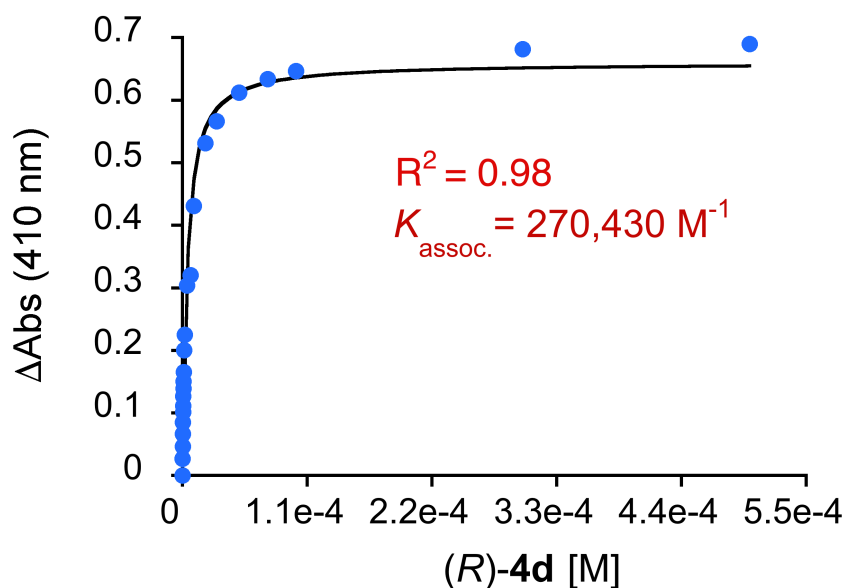


Figure S2. Binding affinity measurement for *R_P-4d* titration with Zn-MAPOL **2**.

Jobs plot analysis: Job's plot analysis was performed by measuring the changes in the UV-vis absorbance of Zn-MAPOL **2** upon addition of *R_P-4d* (Figure-S1). Changes in the UV-vis absorbance (ΔA_{abs}) were calculated by subtracting the absorbance at each titration point from the absorbance of free Zn-MAPOL **2** at 410 nm. The molar fraction of Zn-MAPOL **2** ($X_{\text{Zn-MAPOL}}$) was then multiplied with the change in the UV-vis absorbance (ΔA_{abs}) for each titration point and was plotted against the molar fraction of X_{R-4d} . The maxima at $0.5 X_{R-4d}$ confirms the formation of a 1:1 complex between Zn-MAPOL **2** and phosphine oxide *R_P-4d*.

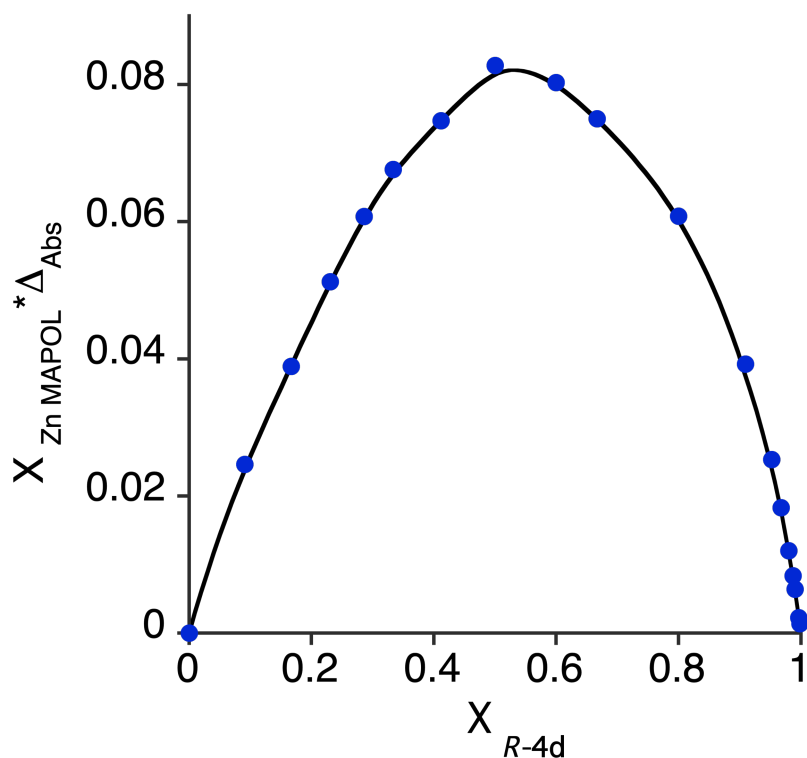


Figure S3. Jobs plot of Zn-MAPOL **2** with *R_P-4d* at 410 nm.

III. General Procedure for CD Measurement:

Zn-MAPOL **2** (1.0 μ L of a 0.001M solution in anhydrous dichloromethane, 1.0 μ mol) was added to hexane (1.0 mL) in a 1.0 cm CD cell (cooled to 0 $^{\circ}$ C) to obtain a 1.0 μ M solution. The background spectrum was recorded from 350 nm to 480 nm with a scan rate of 100 nm/min at 0 $^{\circ}$ C. Chiral phosphine oxide from a stock solution in anhydrous dichloromethane (0.001 M for 1-10 equiv and 0.01 M for 10-20 equiv) was added to the prepared host solution to afford the host-guest complex. The CD spectra were measured immediately (10 scans). The resultant ECCD spectra recorded in millidegrees were converted the molecular CD (Mol. CD) considering the host concentration of 1.0 μ M.

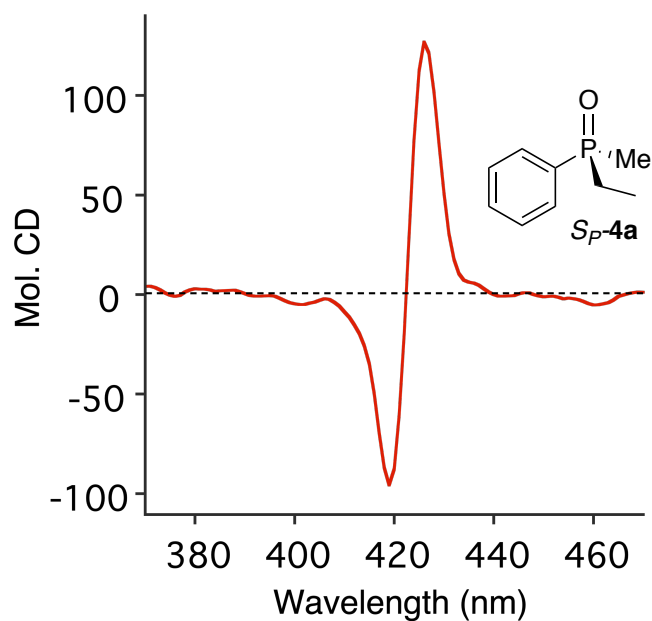


Figure S4. Positive ECCD spectrum of Zn-MAPOL **2** complexed with 5 equiv of *S_P*-**4a** at 0 °C in hexane.

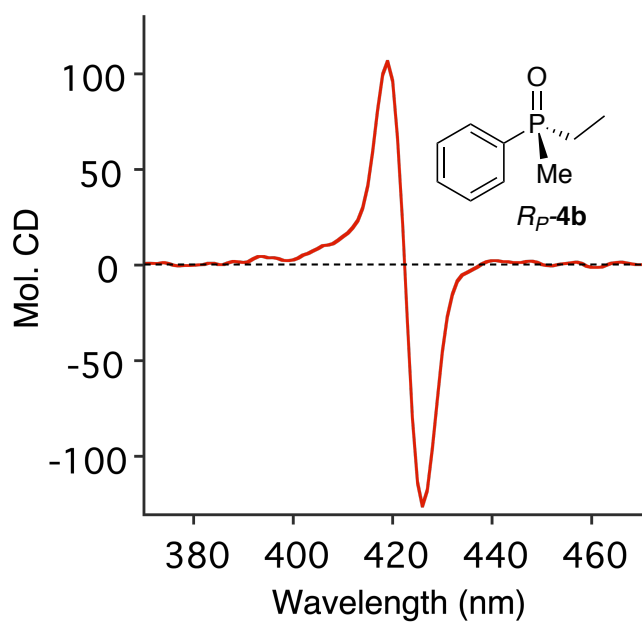


Figure S5. Negative ECCD spectrum of Zn-MAPOL **2** complexed with 5 equiv of *R_P*-**4b** at 0 °C in hexane.

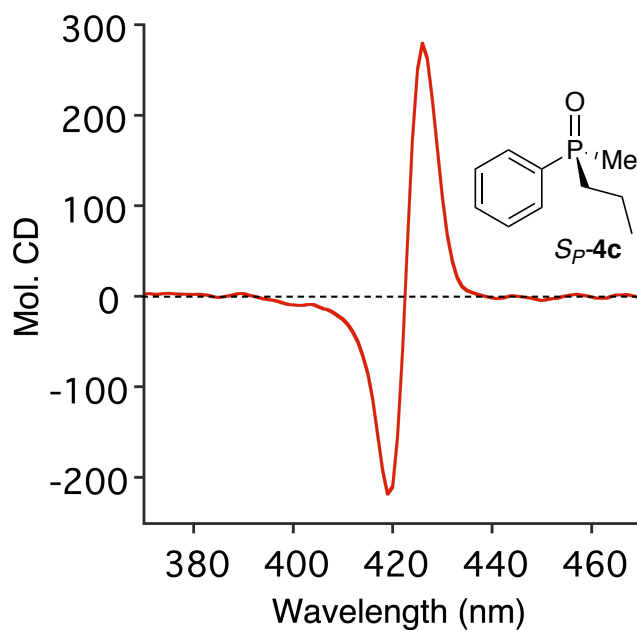


Figure S6. Positive ECCD spectrum of Zn-MAPOL **2** complexed with 5 equiv of *S_P-4c* at 0 °C in hexane.

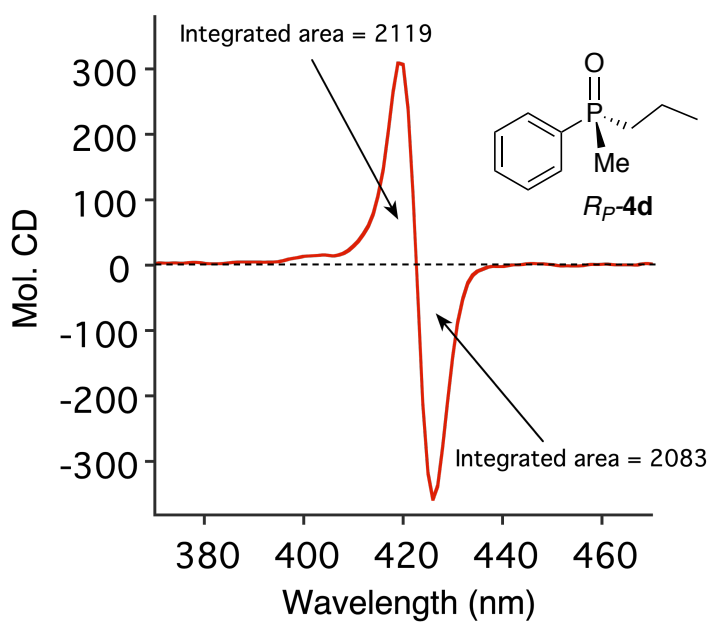


Figure S7. Negative ECCD spectrum of Zn-MAPOL **2** complexed with 5 equiv of *R_P-4d* at 0 °C in hexane.

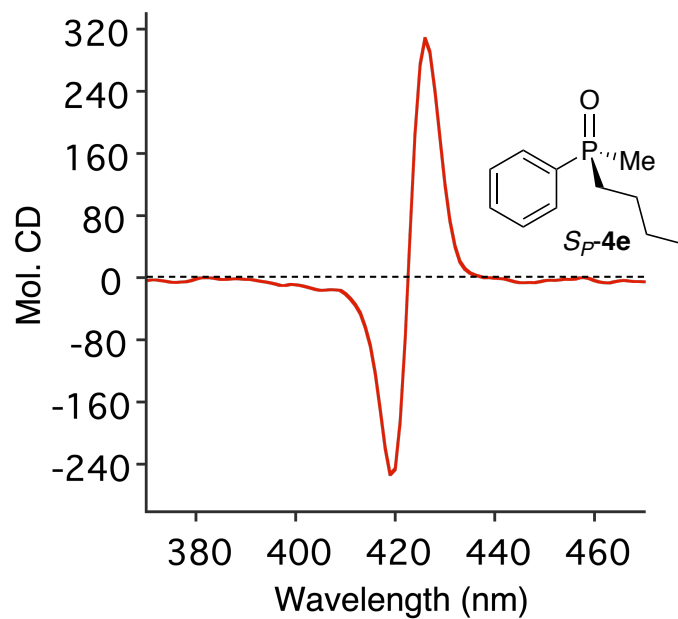


Figure S8. Positive ECCD spectrum of Zn-MAPOL **2** complexed with 5 equiv of *S_P-4e* at 0 °C in hexane.

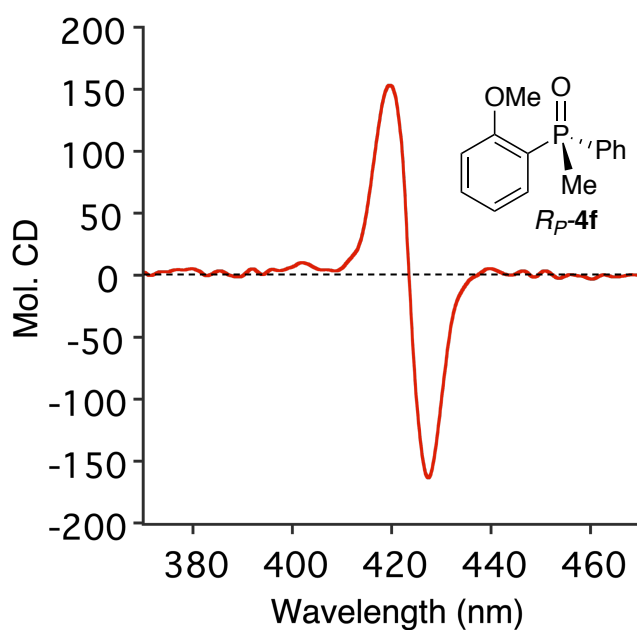


Figure S9. Negative ECCD spectrum of Zn-MAPOL **2** complexed with 5 equiv of *R_P-4f* at 0 °C in hexane.

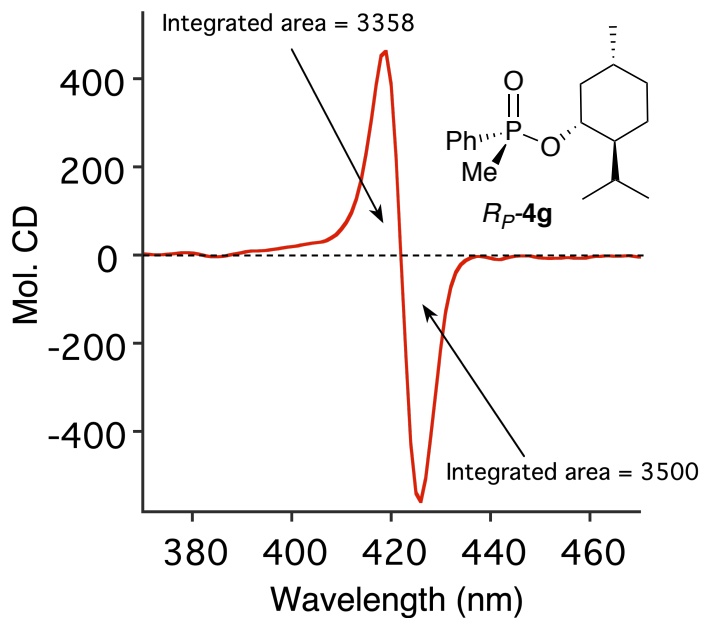


Figure S10. Positive ECD spectrum of Zn-MAPOL **2** complexed with 5 equiv of $R_P\text{-4g}$ at 0 °C in hexane.

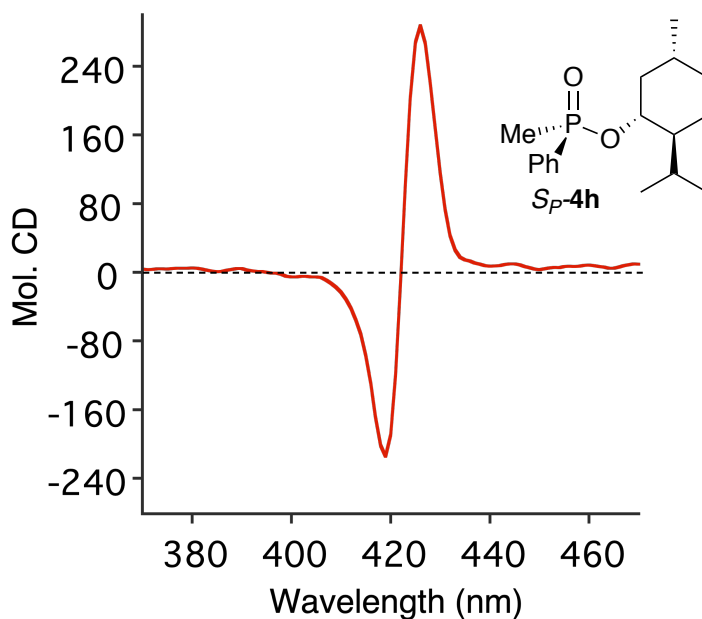


Figure S11. Negative ECD spectrum of Zn-MAPOL **2** complexed with 5 equiv of $S_P\text{-4h}$ at 0 °C in hexane.

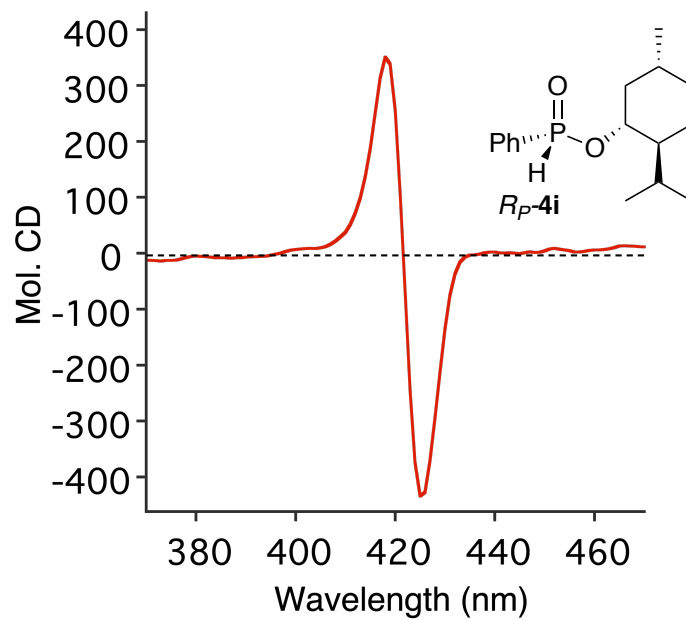


Figure S12. Negative ECCD spectrum of Zn-MAPOL **2** complexed with 5 equiv of *R_P-4i* at 0 °C in hexane.

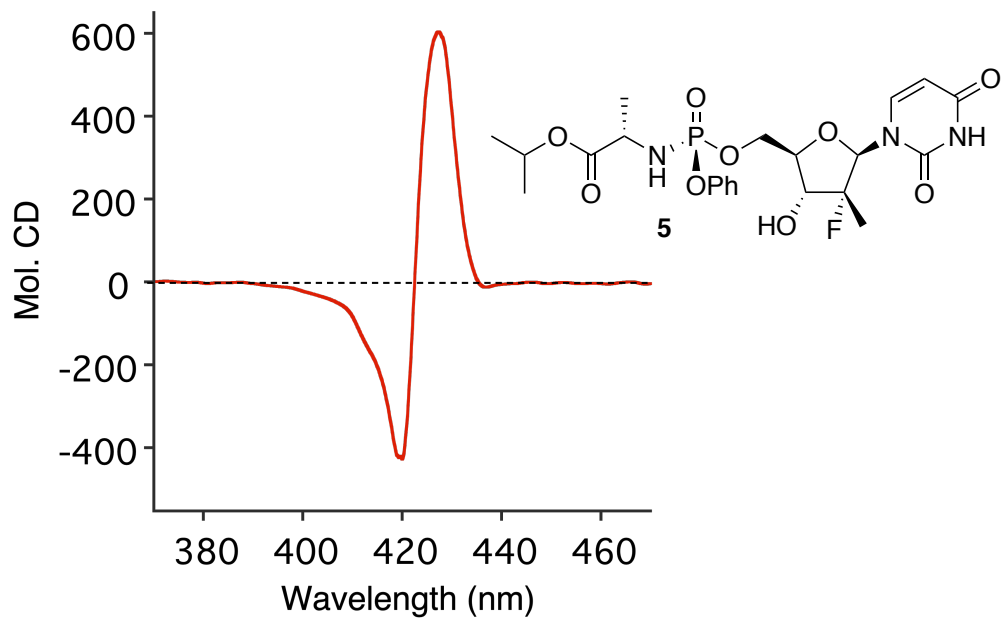


Figure S13. Positive ECCD spectrum of Zn-MAPOL **2** complexed with 1 equiv of **5** at 0 °C in hexane.

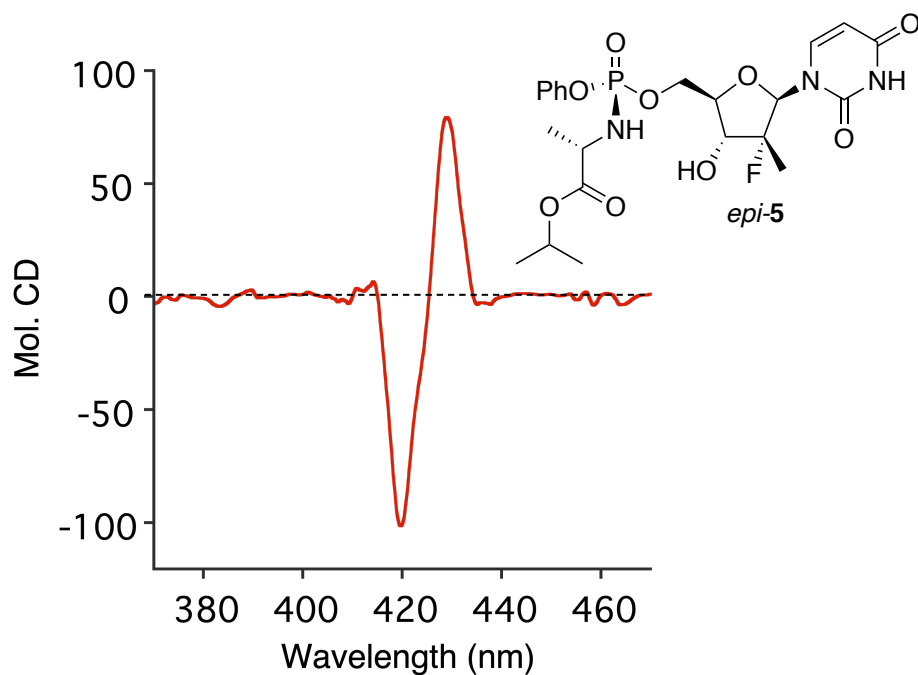


Figure S14. Positive ECCD spectrum of Zn-MAPOL 2 complexed with 1 equiv of *epi-5* at 0 °C in hexane.

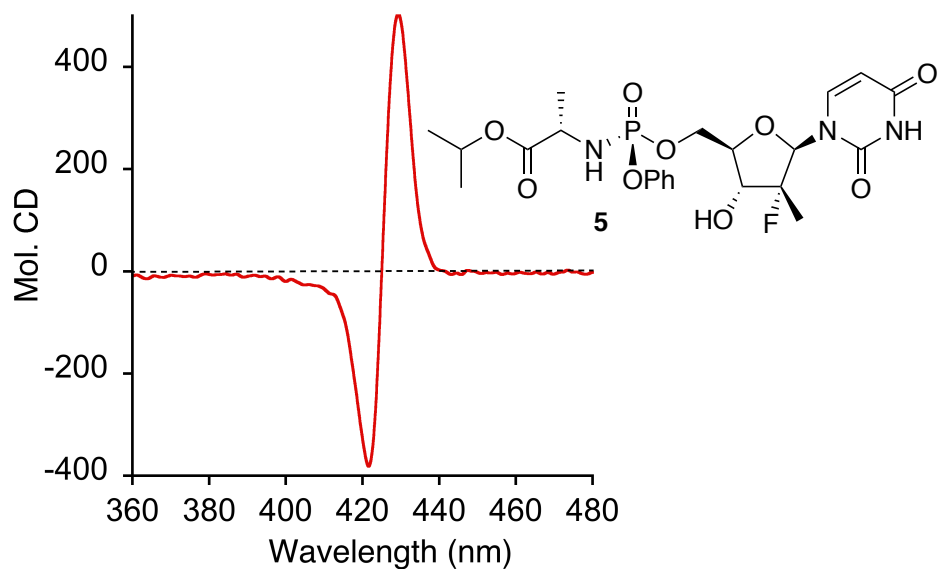


Figure S15. Positive ECCD spectrum of Zn-MAPOL 2 complexed with 20 equiv of **5** at 0 °C in chlorobenzene.

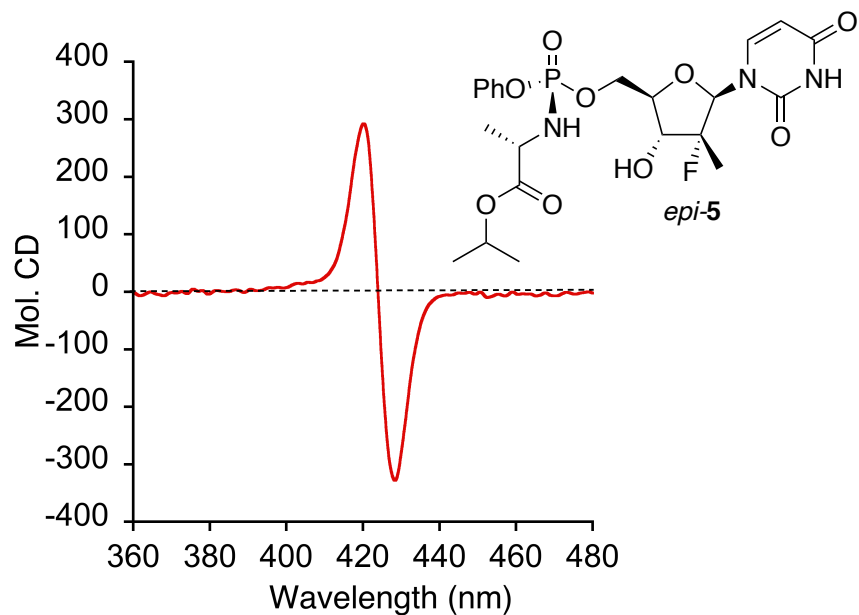


Figure S16. Negative ECCD spectrum of Zn-MAPOL **2** complexed with 20 equiv of *epi-5* at 0 °C in chlorobenzene.

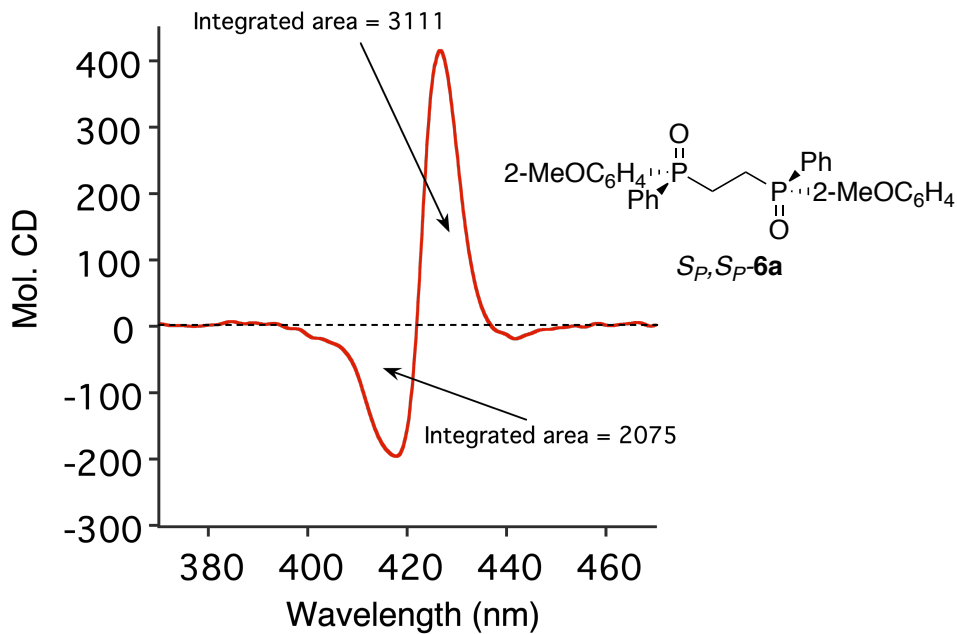


Figure S17. Positive ECCD spectrum of Zn-MAPOL **2** complexed with 1 equiv of S_P, S_P -**6a** at 0 °C in hexane.

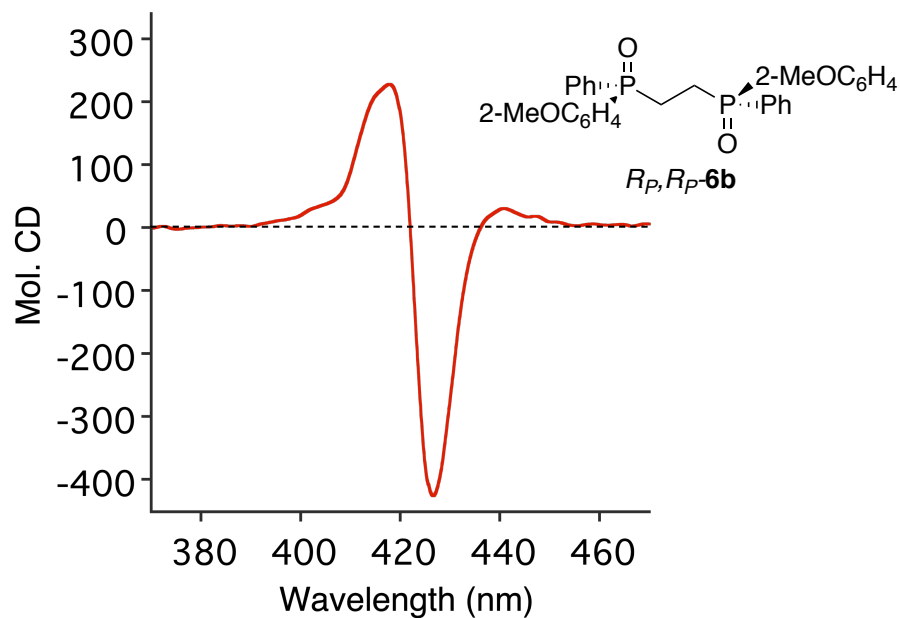


Figure S18. Negative ECCD spectrum of Zn-MAPOL 2 complexed with 1 equiv of R_P,R_P -6b at 0 °C in hexane.

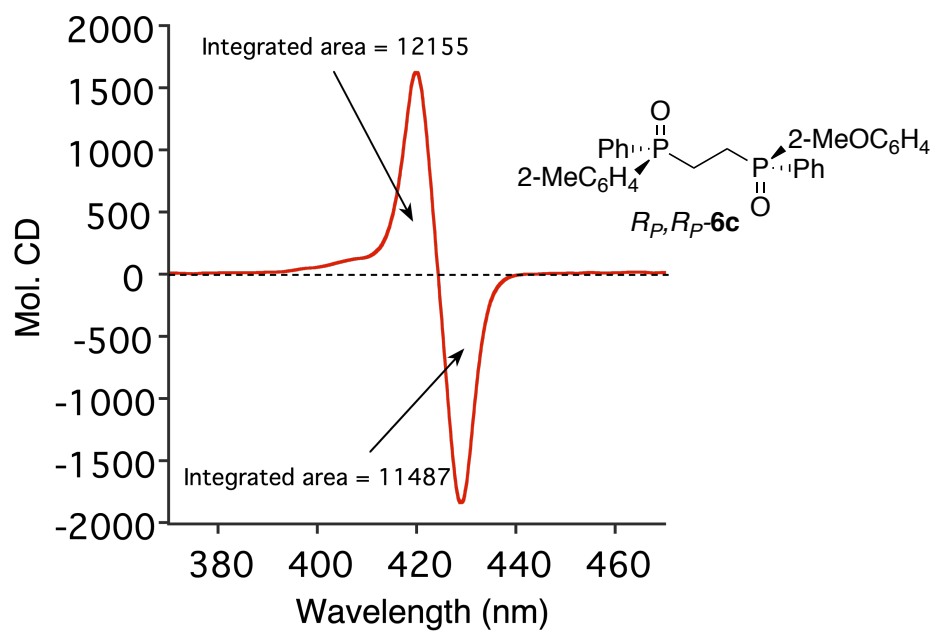


Figure S19. Negative ECCD spectrum of Zn-MAPOL 2 complexed with 1 equiv of R_P,R_P -6c at 0 °C in hexane.

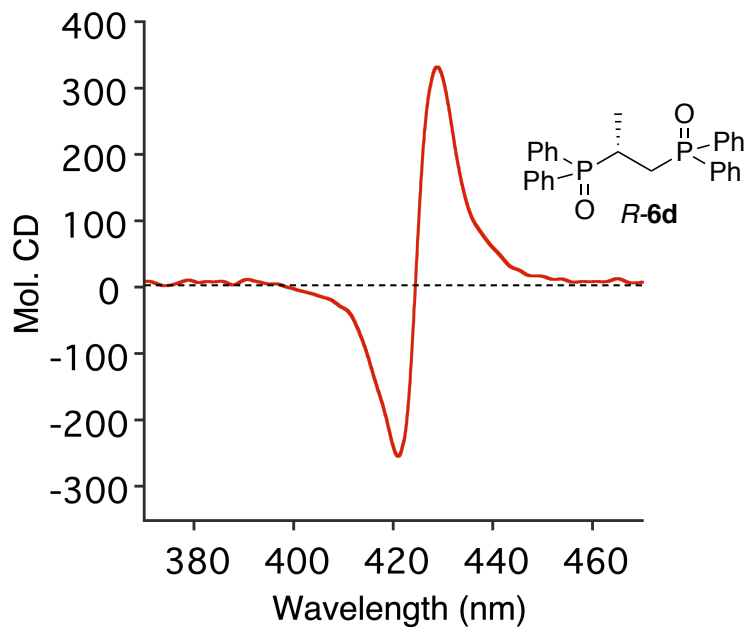


Figure S20. Positive ECCD spectrum of Zn-MAPOL 2 complexed with 1 equiv of *R*-6d at 0 °C in hexane.

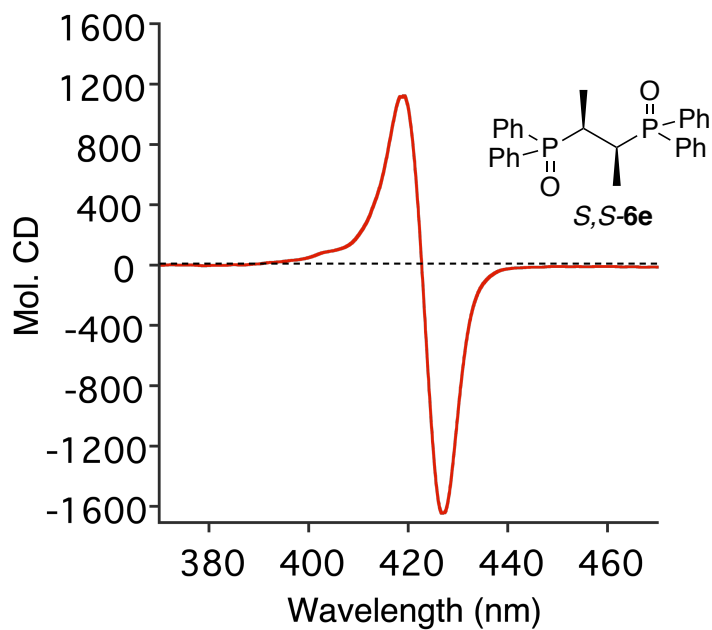


Figure S21. Negative ECCD spectrum of Zn-MAPOL 2 complexed with 1 equiv of *S,S*-6e at 0 °C in hexane.

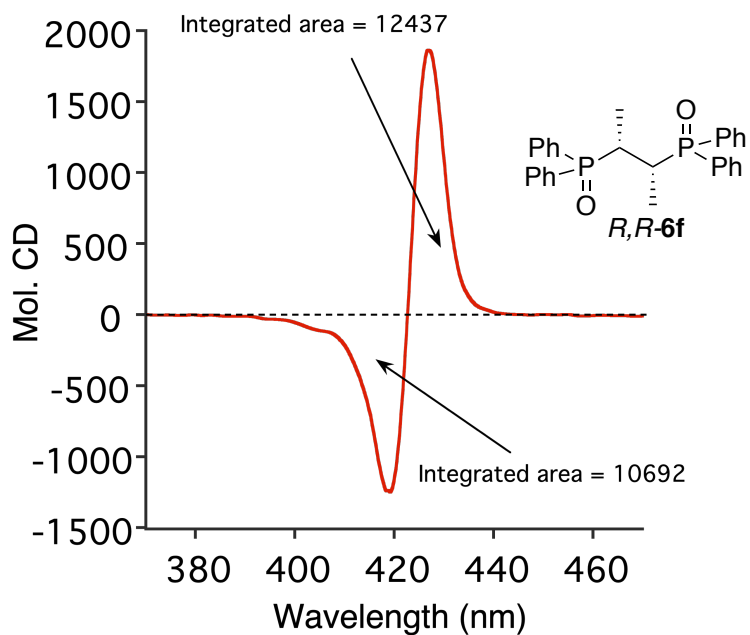


Figure S22. Positive ECCD spectrum of Zn-MAPOL **2** complexed with 1 equiv of *R,R*-**6f** at 0 °C in hexane.

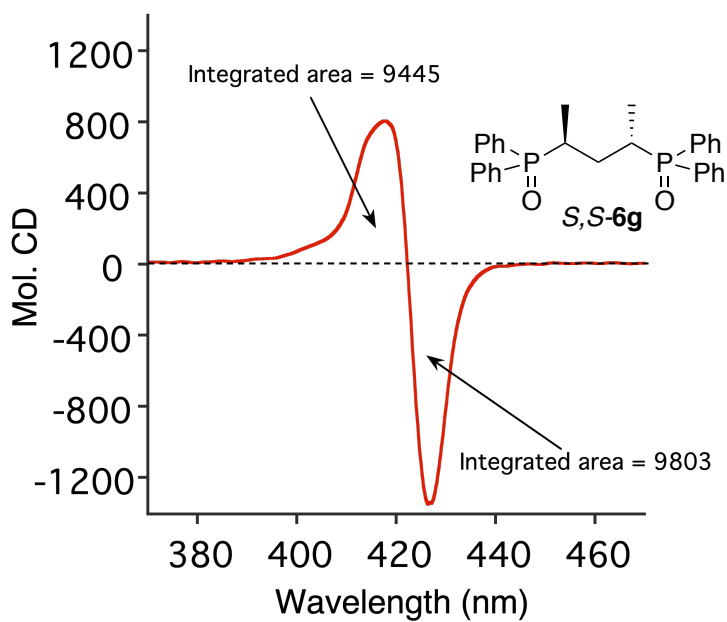


Figure S23. Negative ECCD spectrum of Zn-MAPOL **2** complexed with 1 equiv of *S,S*-**6g** at 0 °C in hexane.

IV. Temperature Dependence on the Amplitude of the ECCD Signal for Zn-MAPOL 2 Complexed with *R_P-4d*

Zn-MAPOL 2 (1.0 μM) was complexed with 5 equiv of *R_P-4d* (5.0 μmol) in hexane. With the increase in temperature the ECCD signal drops gradually, although significant signal is observed even at 45 °C. The same ECCD active solution at 45 °C increases signal intensity when cooled down to 0 °C with an intensity similar to the ECCD signal of the original complex at 0 °C.

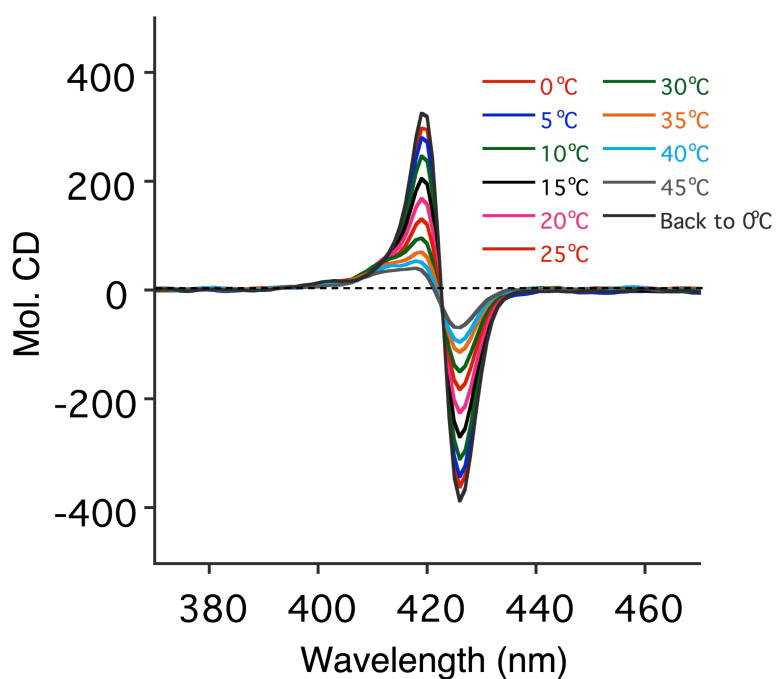


Figure S24. Change in ECCD signal of Zn-MAPOL 2 complexed with 5 equiv of *R_P-4d* in hexane at different temperatures.

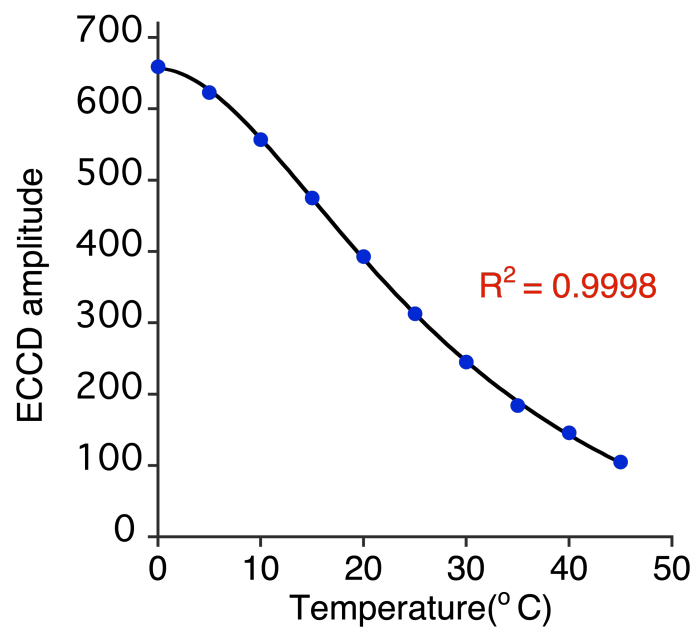


Figure S25. Temperature dependence on the amplitude of the ECCD signal of Zn-MAPOL 2 complexed with 5 equiv of *RP-4d* in hexane.

V. Solvent Screen for Zn-MAPOL 2 Complexed with R_P -4d and R_P -4g

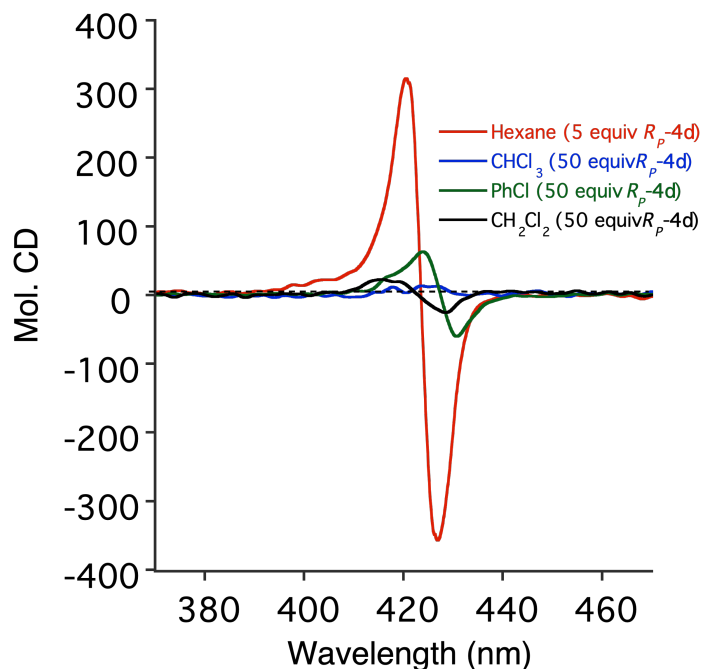


Figure S26. ECCD spectra of Zn-MAPOL 2 complexed with R_P -4d at 0 °C in different

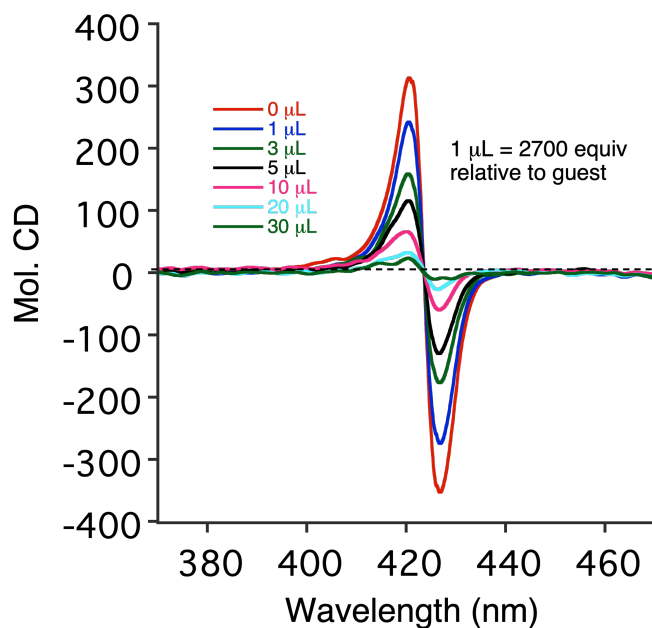


Figure S27. ECCD titration of Zn-MAPOL 2 complexed with 5 equiv of R_P -4d at 0 °C with acetone.

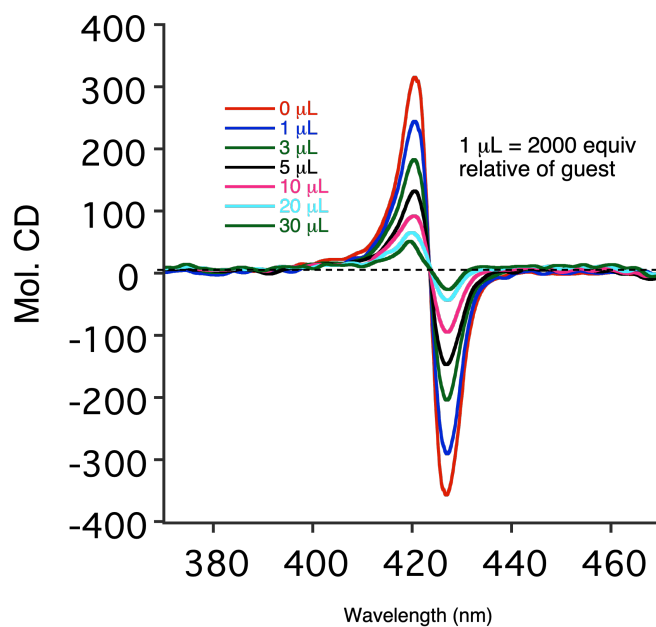


Figure S28. ECCD titration of Zn-MAPOL **2** complexed with 5 equiv of *RP-4d* at 0 °C with ethyl acetate.

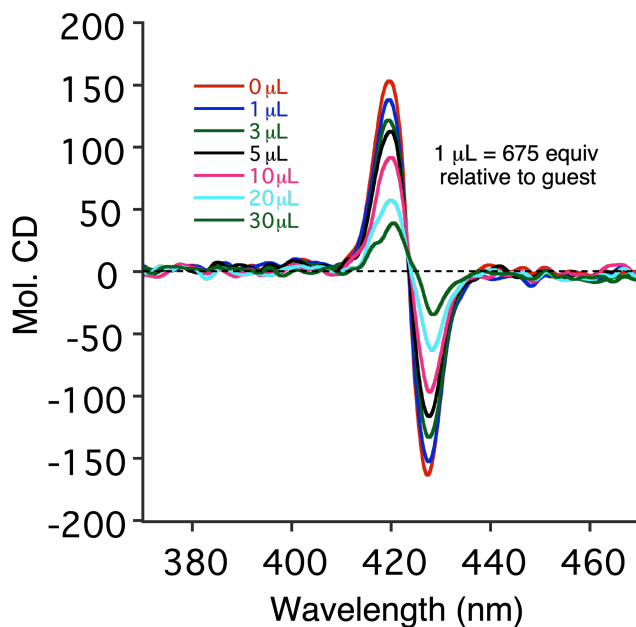


Figure S29. ECCD titration of Zn-MAPOL **2** complexed with 20 equiv of *RP-4g* at 0 °C with acetone.

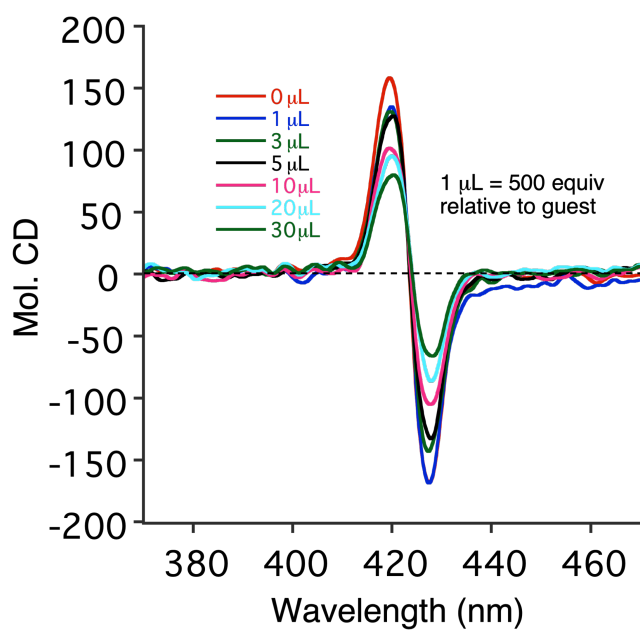


Figure S30. ECCD titration of Zn-MAPOL **2** complexed with 20 equiv of *RP-4g* at 0 °C in ethyl acetate.

VI. ECCD of MeO-Zn-MAPOL 3 Complexed with Chiral Phosphorous Oxide

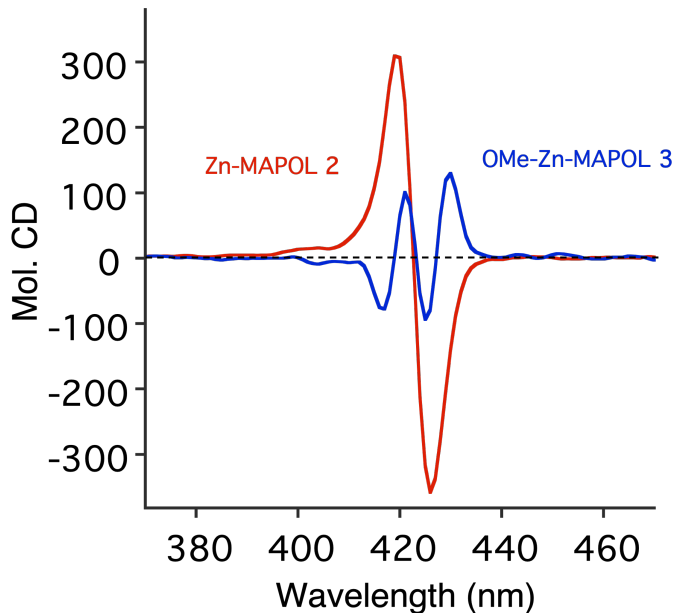


Figure S31. ECCD of Zn-MAPOL **2** (red curve) and MeO-Zn-MAPOL **3** (blue curve) complexed with 5 equiv of *RP-4d* at 0 °C in hexane.

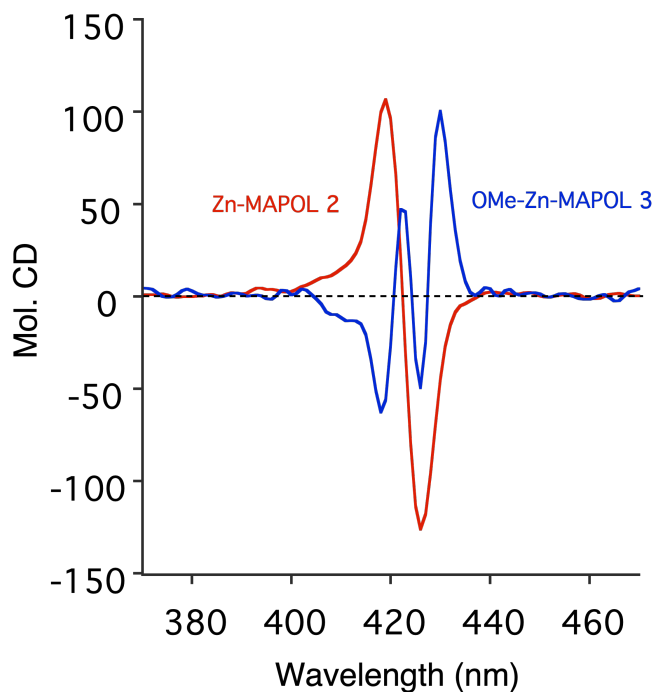


Figure S32. ECCD of Zn-MAPOL **2** (red curve) and MeO-Zn-MAPOL **3** (blue curve) complexed with 5 equiv of *RP-4b* at 0 °C in hexane.

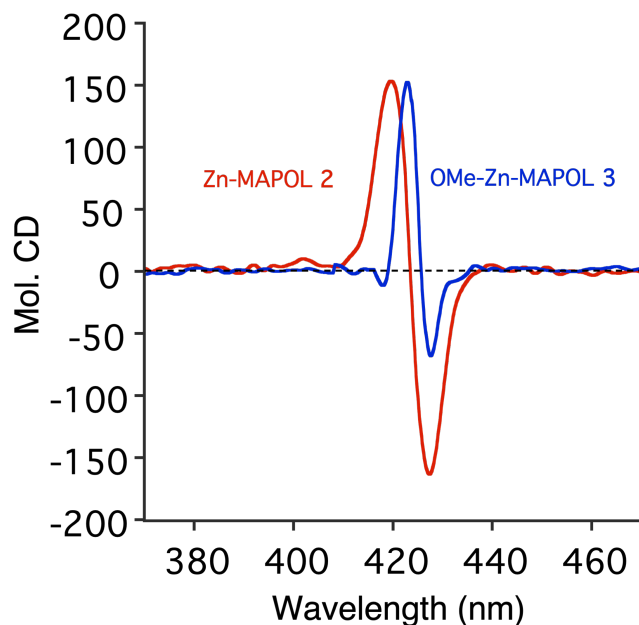


Figure S33. ECCD of Zn-MAPOL **2** (red curve) and MeO-Zn-MAPOL **3** (blue curve) complexed with 20 equiv of *R_P*-**4f** at 0 °C in hexane.

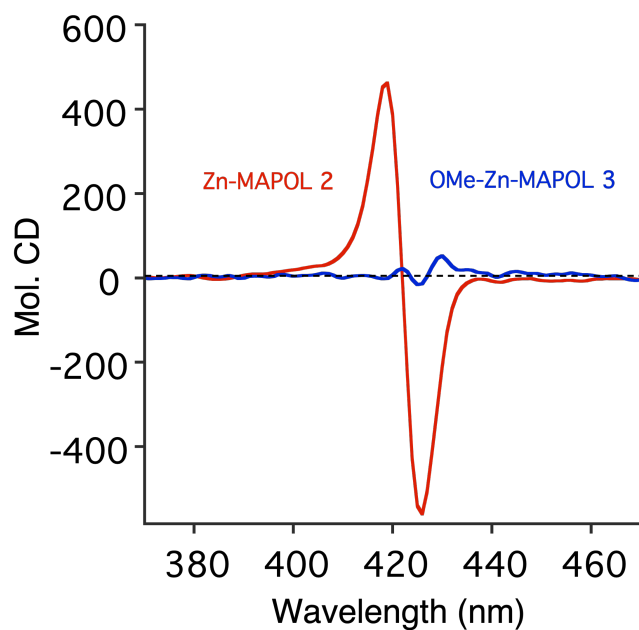


Figure S34. ECCD of Zn-MAPOL **2** (red curve) and MeO-Zn-MAPOL **3** (blue curve) complexed with 5 equiv of *R_P*-**4g** at 0 °C in hexane.

VII. Experimental Procedure:

P-chiral phosphine oxides were synthesized following literature procedures.² Optical purity was measured comparing their optical rotation values with the reported values.

ethyl(methyl)(phenyl)phosphine oxide:^{2a,2b,3}



S_P-**4a** enantiomer:

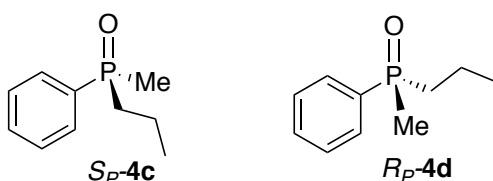
$[\alpha]_D = -16.7$ ($c = 1.0$, MeOH); $ee = 68\%$

R_P-**4b** enantiomer:

$[\alpha]_D = +18.1$ ($c = 1.0$, MeOH); $ee = 74\%$

¹H NMR (500 MHz, CDCl₃) δ 7.72 – 7.67 (m, 2H), 7.54 – 7.46 (m, 3H), 2.03 – 1.83 (m, 2H), 1.69 (dd, $J = 12.7, 1.4$ Hz, 3H), 1.15 – 1.08 (m, 3H). ¹³C NMR (126 MHz, CDCl₃) δ 133.62, 132.86, 131.61 (d, $J = 2.7$ Hz), 130.07 (d, $J = 9.3$ Hz), 128.64 (d, $J = 11.4$ Hz), 24.64 (d, $J = 71.4$ Hz), 15.40 (d, $J = 69.6$ Hz), 5.73 (d, $J = 5.1$ Hz). ³¹P NMR (202 MHz, CDCl₃) δ 39.11.

methyl(phenyl)(propyl)phosphine oxide:^{2b,3}



***S_P*-4c** enantiomer:

$[\alpha]_D = -13.2$ ($c = 1.0$, MeOH); $ee = 78\%$

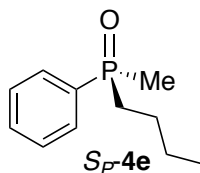
***R_P*-4d** enantiomer:

$[\alpha]_D = +15.5$ ($c = 1.0$, MeOH); $ee = 92\%$

^1H NMR (500 MHz, CDCl_3) δ 7.73 – 7.69 (m, 2H), 7.53 – 7.48 (m, 3H), 2.00 – 1.81 (m, 3H), 1.69 (d, $J = 12.7$ Hz, 3H), 1.67 – 1.47 (m, 2H), 0.99 (td, $J = 7.3, 1.1$ Hz, 3H).

^{13}C NMR (126 MHz, CDCl_3) δ 134.15, 133.99, 131.55 (d, $J = 2.6$ Hz), 129.99 (d, $J = 9.3$ Hz), 128.63 (d, $J = 11.4$ Hz), 33.91 (d, $J = 70.4$ Hz), 16.32, 15.73 (d, $J = 11.9$ Hz), 15.56, 15.42 (d, $J = 3.8$ Hz). ^{31}P NMR (202 MHz, CDCl_3) δ 37.11.

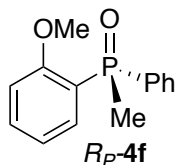
butyl(methyl)(phenyl)phosphine oxide:^{2a,2b,4}



$[\alpha]_D = -11.5$ ($c = 1.0$, MeOH); $ee = 69\%$

^1H NMR (500 MHz, CDCl_3) δ 7.70 – 7.67 (m, 2H), 7.59 – 7.41 (m, 3H), 2.02 – 1.81 (m, 2H), 1.70 (d, $J = 12.7$ Hz, 3H), 1.66 – 1.42 (m, 2H), 1.42 – 1.32 (m, 2H), 0.87 (t, $J = 7.3$ Hz, 3H). ^{13}C NMR (126 MHz, CDCl_3) δ 134.16, 133.40, (131.55 (d, $J = 2.8$ Hz), 130.02 (d, $J = 9.1$ Hz), 128.64 (d, $J = 11.4$ Hz), 31.52 (d, $J = 70.5$ Hz), 24.03 (d, $J = 15.2$ Hz), 23.68 (d, $J = 4.3$ Hz), 16.04 (d, $J = 69.5$ Hz), 13.58. ^{31}P NMR (202 MHz, CDCl_3) δ 37.39

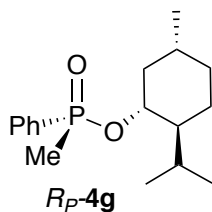
2-methoxyphenyl(methyl)(phenyl)phosphine oxide:^{2a,2b}



$[\alpha]_D = +18.8$ ($c = 1.0$, MeOH); $ee = 71\%$

^1H NMR (500 MHz, CDCl_3) δ 7.97 (ddd, $J = 13.1, 7.5, 1.8$ Hz, 1H), 7.79 – 7.68 (m, 2H), 7.55 – 7.45 (m, 2H), 7.44 – 7.40 (m, 2H), 7.11 (tdd, $J = 7.5, 1.8, 0.9$ Hz, 1H), 6.89 (ddd, $J = 8.5, 5.4, 0.9$ Hz, 1H), 3.73 (s, 3H), 2.08 (d, $J = 14.0$ Hz, 3H). ^{13}C NMR (126 MHz, CDCl_3) δ 133.97 (d, $J = 6.1$ Hz), 133.88 (d, $J = 2.8$ Hz), 131.25 (d, $J = 2.9$ Hz), 130.26 (d, $J = 10.4$ Hz), 128.20 (d, $J = 12.4$ Hz), 121.04 (d, $J = 11.3$ Hz), 110.84 (d, $J = 6.6$ Hz), 55.28, 16.17 (d, $J = 75.2$ Hz). ^{31}P NMR (202 MHz, CDCl_3) δ 28.33.

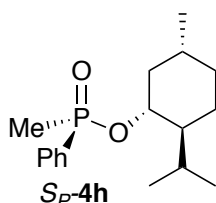
(1*R*,2*S*,5*R*)-2-isopropyl-5-methylcyclohexyl (*R*_P)-methyl(phenyl) phosphinate:^{3,5}



^1H NMR (500 MHz, CDCl_3) δ 7.85 – 7.75 (m, 2H), 7.56 – 7.50 (m, 1H), 7.49 – 7.44 (m, 2H), 4.27 (tdd, $J = 10.7, 8.2, 4.5$ Hz, 1H), 2.23 – 2.17 (m, 1H), 1.83–1.79 (m, 1H), 1.71 – 1.55 (m, 5H), 1.39 – 1.29 (m, 2H), 1.04 – 0.97 (m, 2H), 0.96 (d, $J = 7.1$ Hz, 3H), 0.88 (d, $J = 6.9$ Hz, 3H), 0.85 – 0.79 (m, 1H), 0.76 (d, $J = 6.6$ Hz, 3H). ^{13}C NMR (126 MHz, CDCl_3) δ 131.89 (d, $J = 2.8$ Hz), 130.82 (d, $J = 10.1$ Hz), 128.40 (d, $J = 12.8$ Hz), 76.37 (d, $J =$

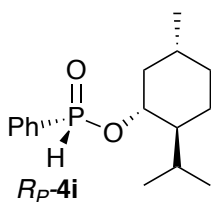
7.1 Hz), 48.75 (d, $J = 6.2$ Hz), 43.21, 34.09, 31.43, 25.85, 22.95, 21.91, 21.10, 16.95, 16.14, 15.83. ^{31}P NMR (202 MHz, CDCl_3) δ 39.81.

(1*R*,2*S*,5*R*)-2-isopropyl-5-methylcyclohexyl (*S_P*)-methyl(phenyl) phosphinate:^{2c,3,5}



^1H NMR (500 MHz, CDCl_3) δ 7.83 – 7.79 (m, 2H), 7.58 – 7.51 (m, 1H), 7.51 – 7.45 (m, 2H), 3.97 (tdd, $J = 10.5, 7.9, 4.5$ Hz, 1H), 2.45 – 2.33 (m, 1H), 1.94 – 1.88 (m, 1H), 1.72 (d, $J = 14.5$ Hz, 3H), 1.65 – 1.55 (m, 2H), 1.43 – 1.37 (m, 1H), 1.35 – 1.19 (m, 3H), 0.92 (d, $J = 6.5$ Hz, 3H), 0.86 (d, $J = 10.3$ Hz, 1H), 0.83 (d, $J = 7.1$ Hz, 1H), 0.31 (d, $J = 6.9$ Hz, 3H). ^{13}C NMR (126 MHz, CDCl_3) δ 131.97 (d, $J = 2.6$ Hz), 131.12 (d, $J = 10.0$ Hz), 128.41 (d, $J = 12.8$ Hz), 76.69, 48.76 (d, $J = 6.8$ Hz), 43.87, 34.07, 31.54, 25.36, 22.67, 21.98, 21.08, 16.96, 16.14, 15.15. ^{31}P NMR (202 MHz, CDCl_3) δ 40.49. $dr = 12.5 : 1$

(1*R*,2*S*,5*R*)-2-isopropyl-5-methylcyclohexyl (*R_P*)-phenyl phosphinate:^{2c}



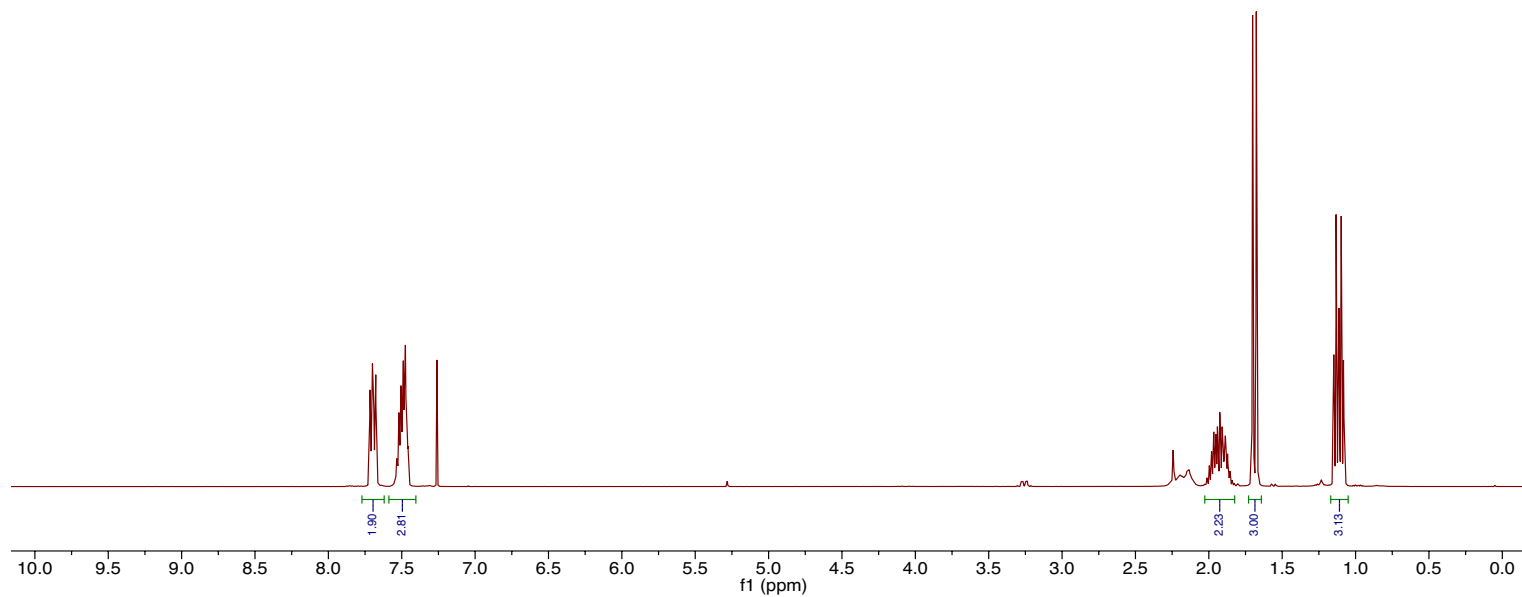
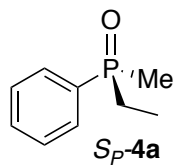
^1H NMR (500 MHz, CDCl_3) δ 8.20 (s, 1H), 7.80 – 7.75 (m, 2H), 7.65 (d, $J_{\text{HP}} = 550$ Hz, 1H), 7.60 – 7.57 (m, 1H), 7.52 – 7.48 (m, 2H), 4.25 (qd, $J = 10.5, 4.5$ Hz, 1H), 2.24 – 2.15

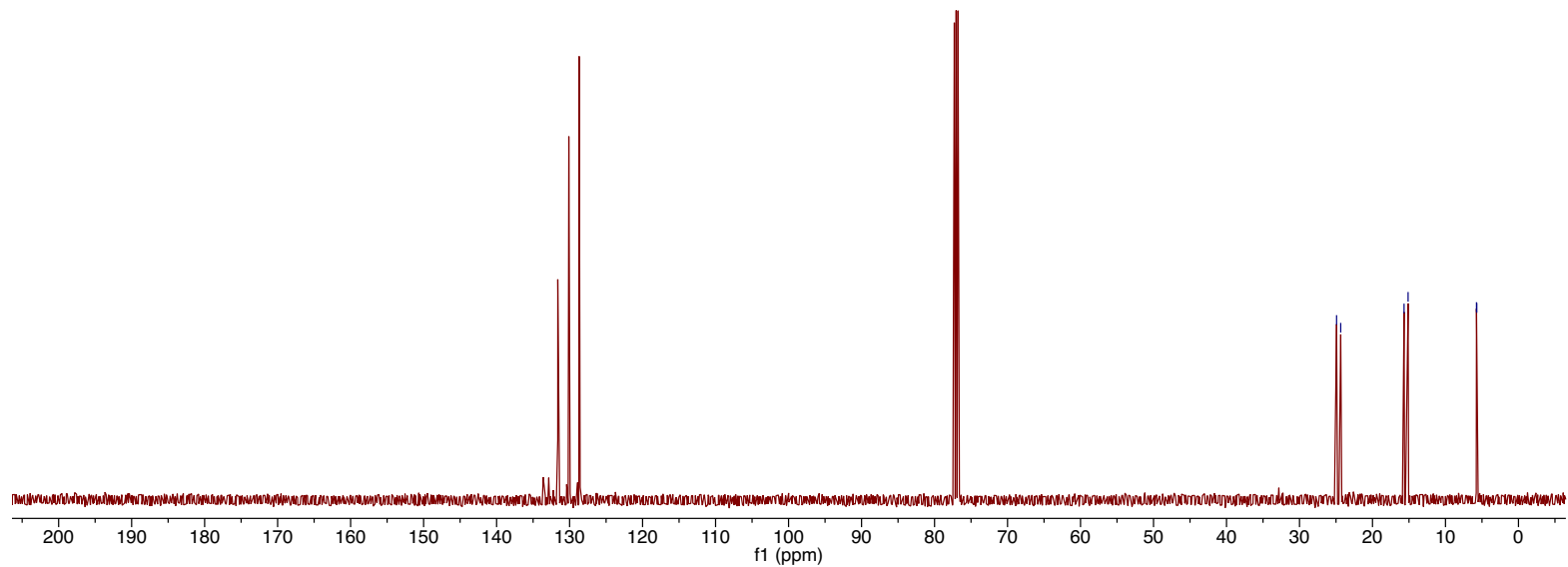
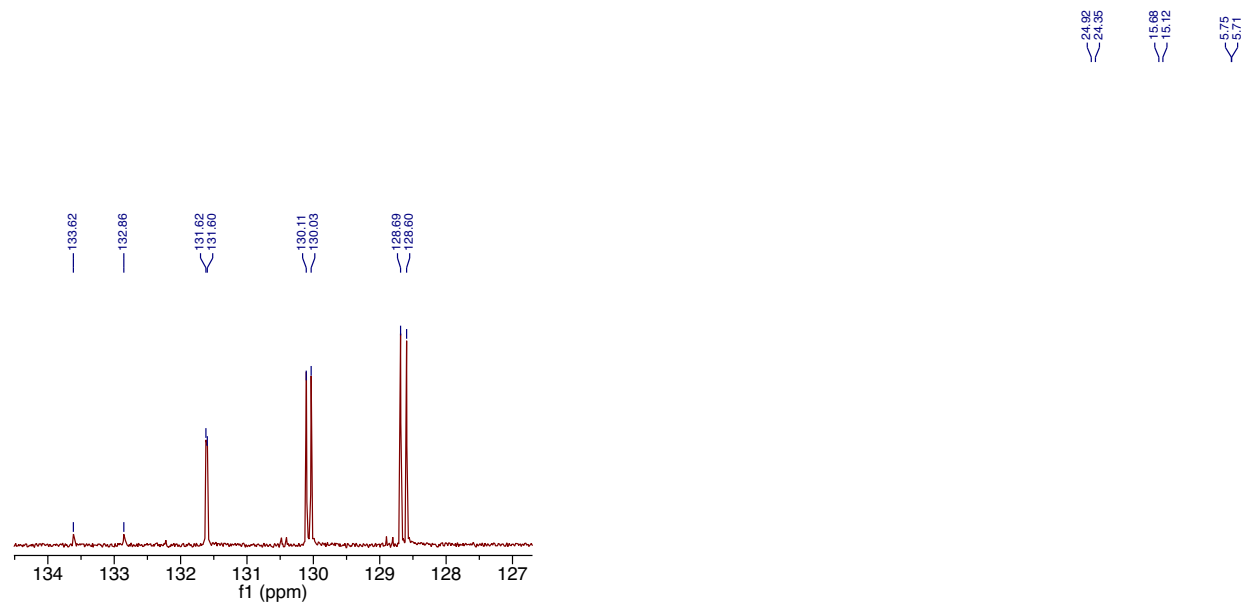
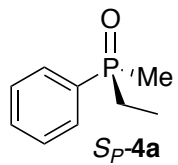
(m, 2H), 1.71 – 1.65 (m, 2H), 1.48 – 1.42 (m, 2H), 1.24 (q, $J = 10.0$ Hz, 1H), 1.04 (qd, , $J = 15$ Hz, 5 Hz, 1H), 0.95 (d, $J = 7.0$ Hz, 3H), 0.87 (m, 7H), ^{13}C NMR (126 MHz, CDCl_3) δ 132.91 (d, $J = 2.9$ Hz), 130.63, (d, $J = 11.8$ Hz), 128.67 (d, $J = 13.8$ Hz), 78.96 (d, $J = 7.4$ Hz), 48.69 (d, $J = 6.2$ Hz), 43.49 (d, $J = 1.1$ Hz), 33.91, 31.63, 25.76, 22.89, 21.86, 20.99, 15.73. ^{31}P NMR (202 MHz, CDCl_3) δ 24.73. $dr = 19 : 1$

IX. References:

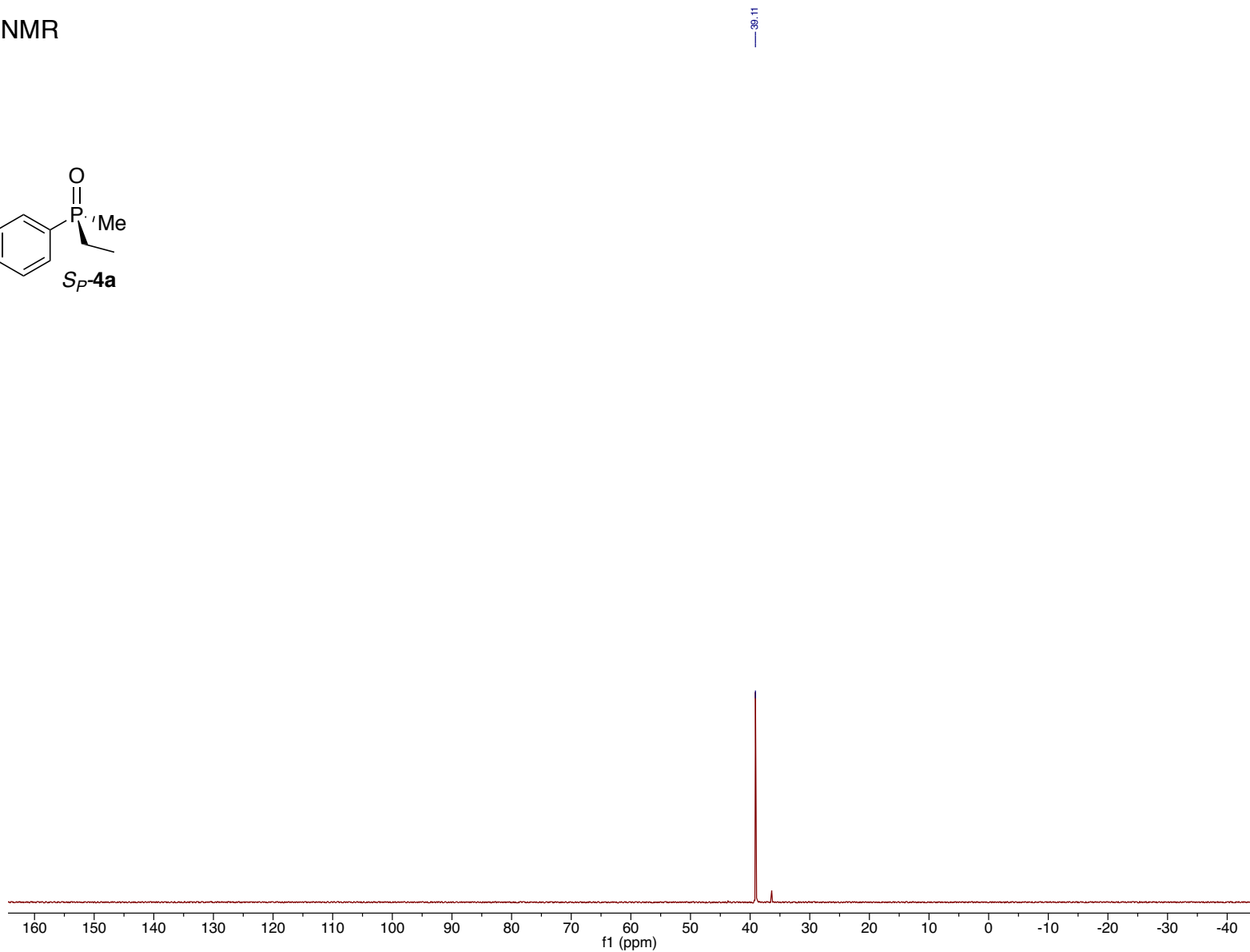
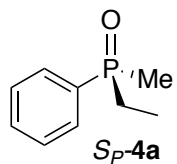
- (1) Shoji, Y.; Tashiro, K.; Aida, T. Sensing of chiral fullerenes by a cyclic host with an asymmetrically distorted pi-electronic component. *J. Am. Chem. Soc.* **2006**, *128*, 10690.
- (2) (a) Adams, H.; Collins, R. C.; Jones, S.; Warner, C. J. A. Enantioselective Preparation of P-Chiral Phosphine Oxides. *Org. Lett.* **2011**, *13*, 6576; (b) Fernandez, I.; Khair, N.; Roca, A.; Benabra, A.; Alcludia, A.; Espartero, J. L.; Alcludia, F. A generalization of the base effect on the diastereoselective synthesis of sulfinic and phosphinic esters. *Tetrahedron Lett.* **1999**, *40*, 2029; (c) Xu, Q.; Zhao, C. Q.; Han, L. B. Stereospecific nucleophilic substitution of optically pure H-phosphinates: a general way for the preparation of chiral P-stereogenic phosphine oxides. *J. Am. Chem. Soc.* **2008**, *130*, 12648.
- (3) Korpiun, O.; Lewis, R. A.; Chickos, J.; Mislow, K. Synthesis and Absolute Configuration of Optically Active Phosphine Oxides and Phosphinates. *J. Am. Chem. Soc.* **1968**, *90*, 4842.
- (4) Segi, M.; Nakamura, Y.; Nakajima, T.; Suga, S. Preparation of Optically-Active Phosphine Oxides by Regioselective Cleavage of Cyclic Phenylphosphonite with Alkyl-Halides. *Chem. Lett.* **1983**, 913.
- (5) Korpiun, O.; Mislow, K. A New Route to Preparation and Configurational Correlation of Optically Active Phosphine Oxides. *J. Am. Chem. Soc.* **1967**, *89*, 4784.

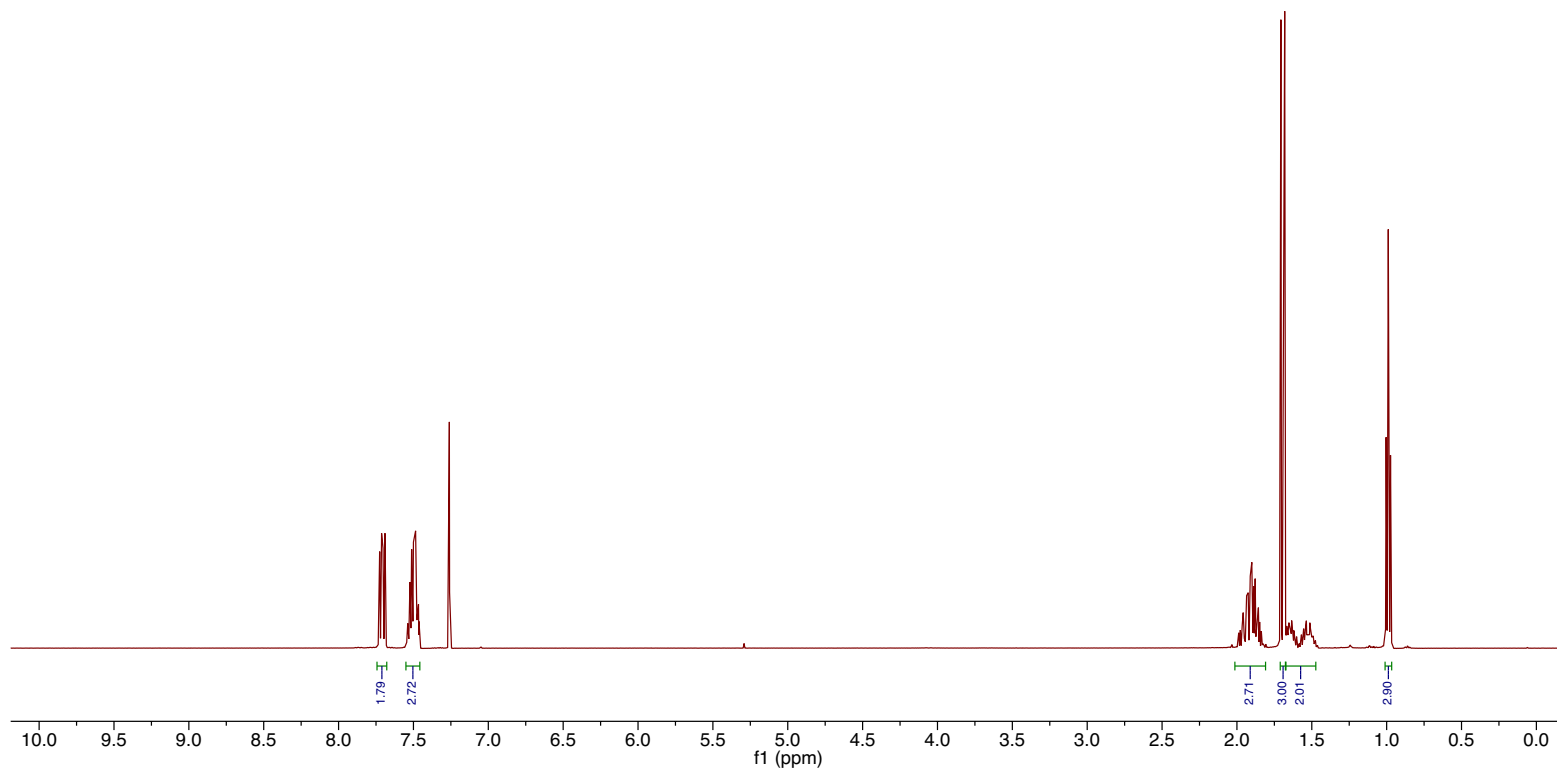
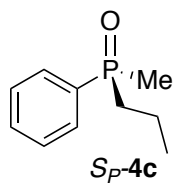
X. NMR Spectra:

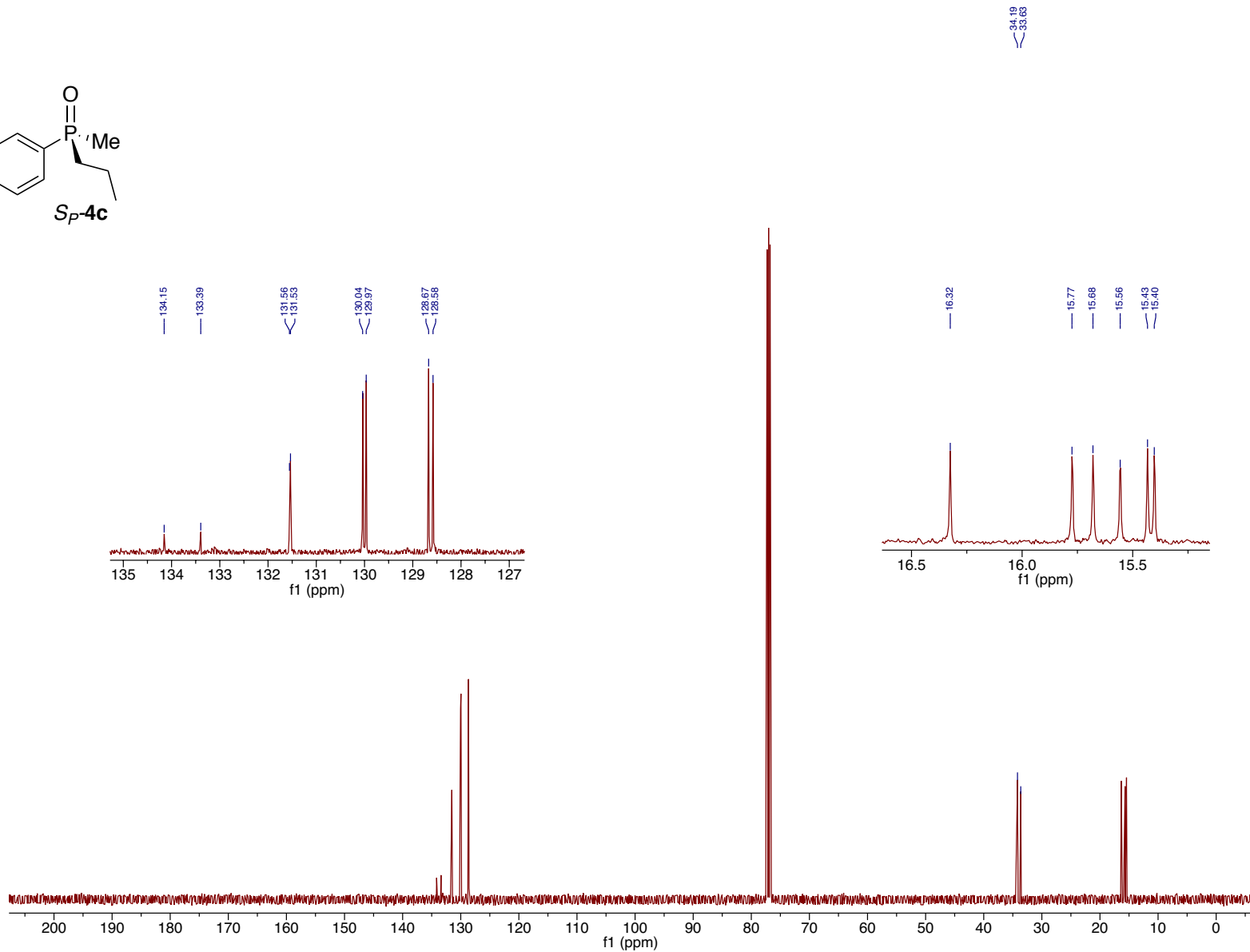
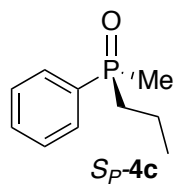




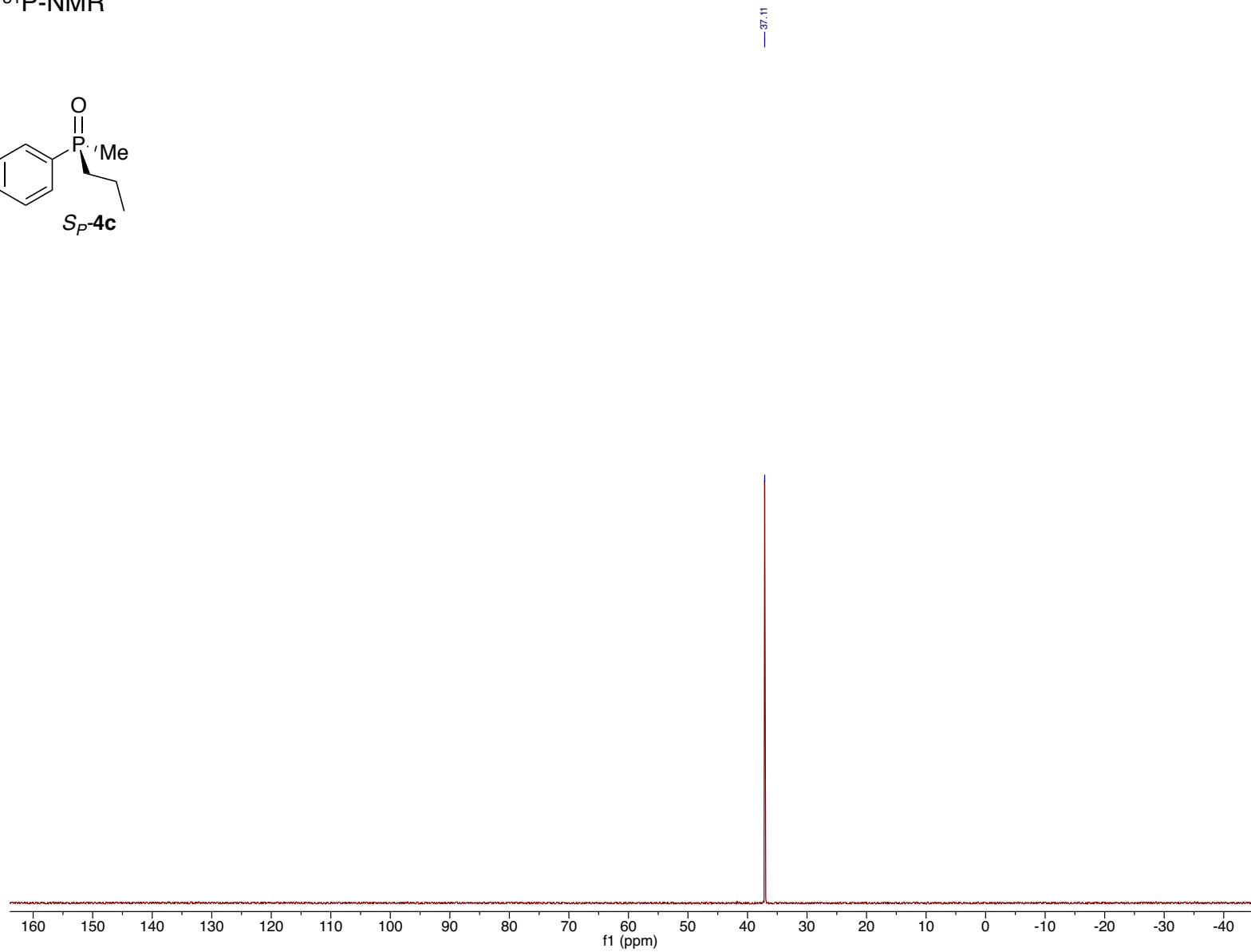
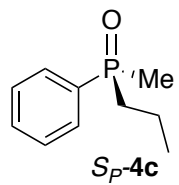
³¹P-NMR

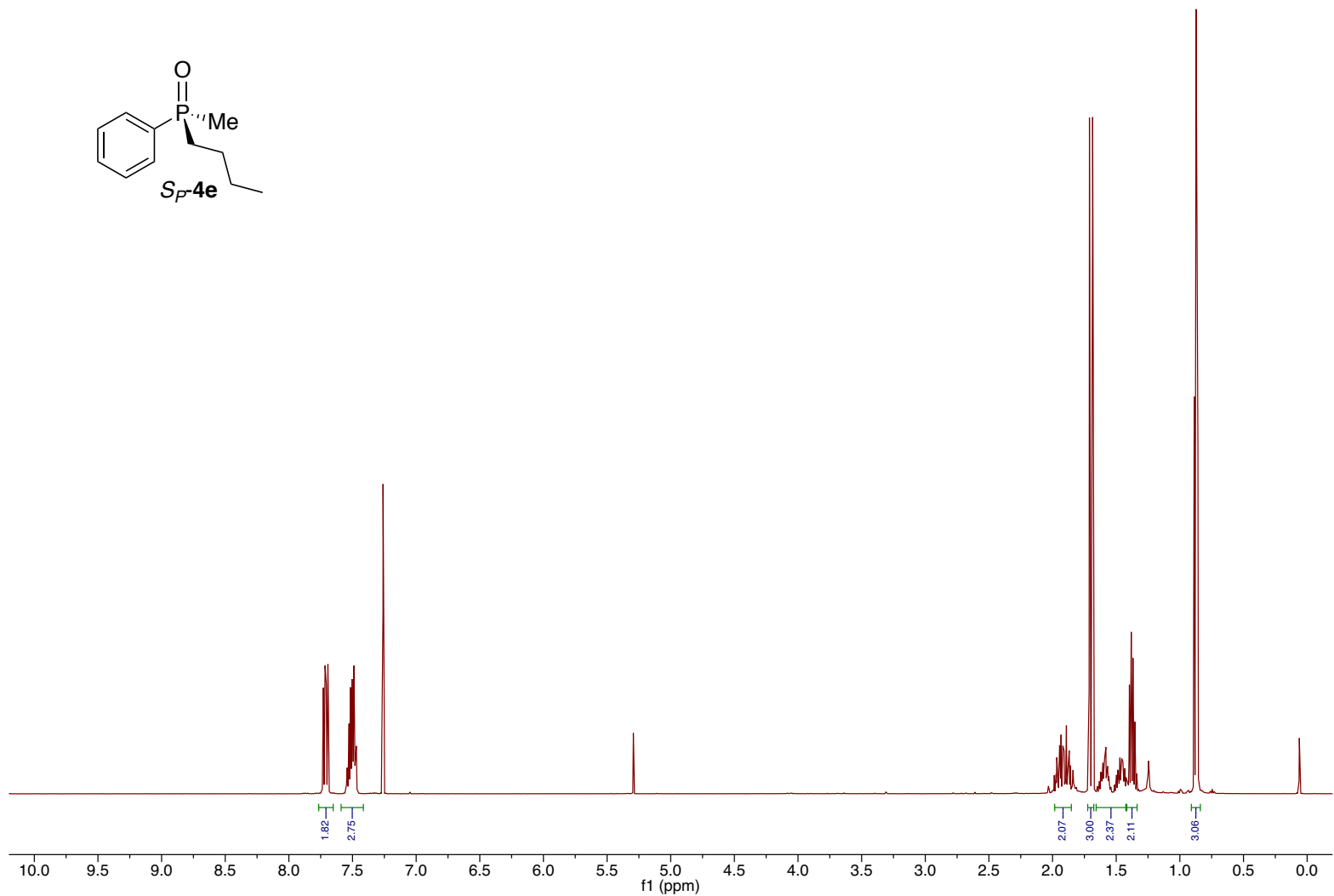
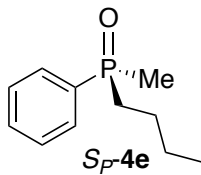


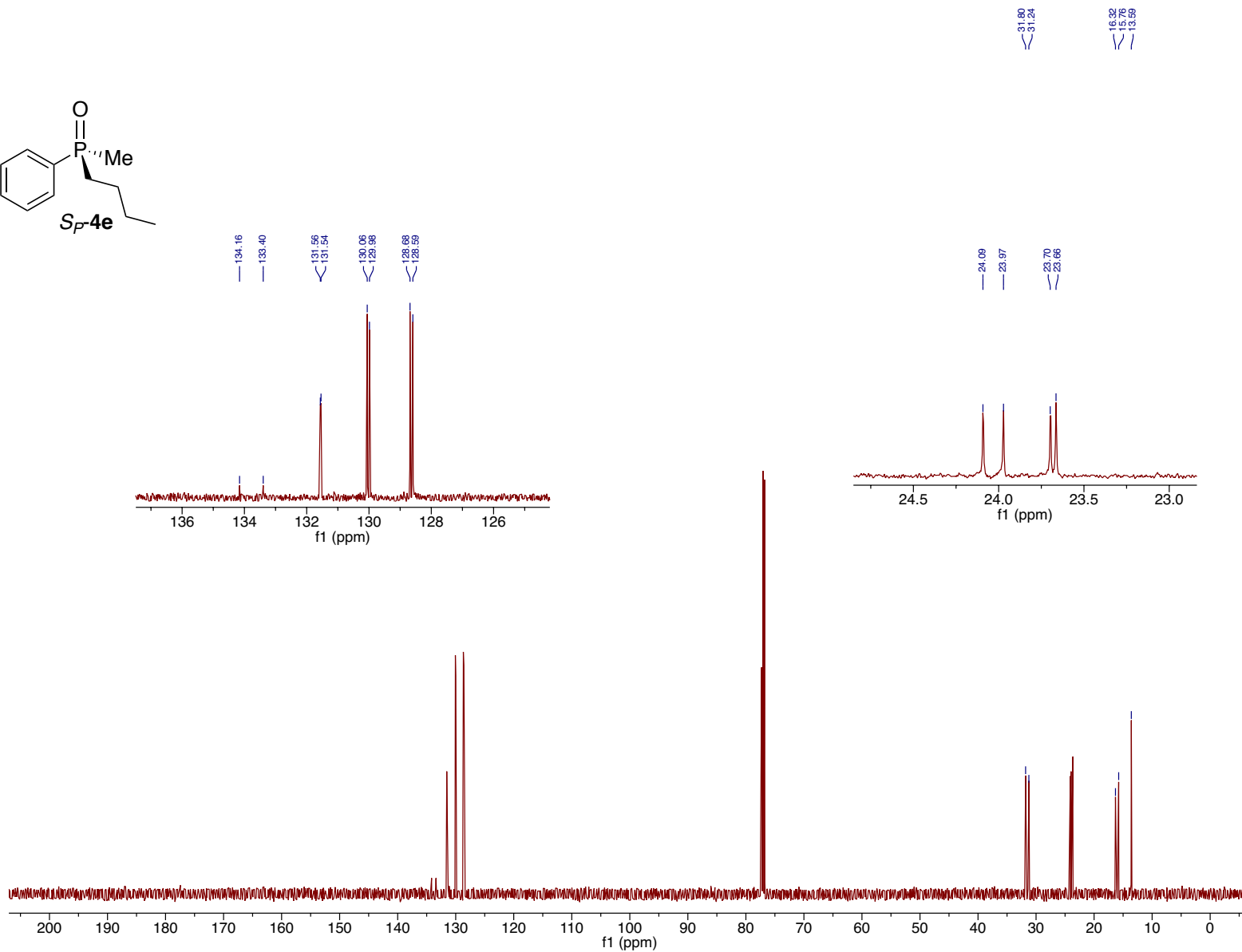
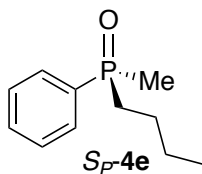




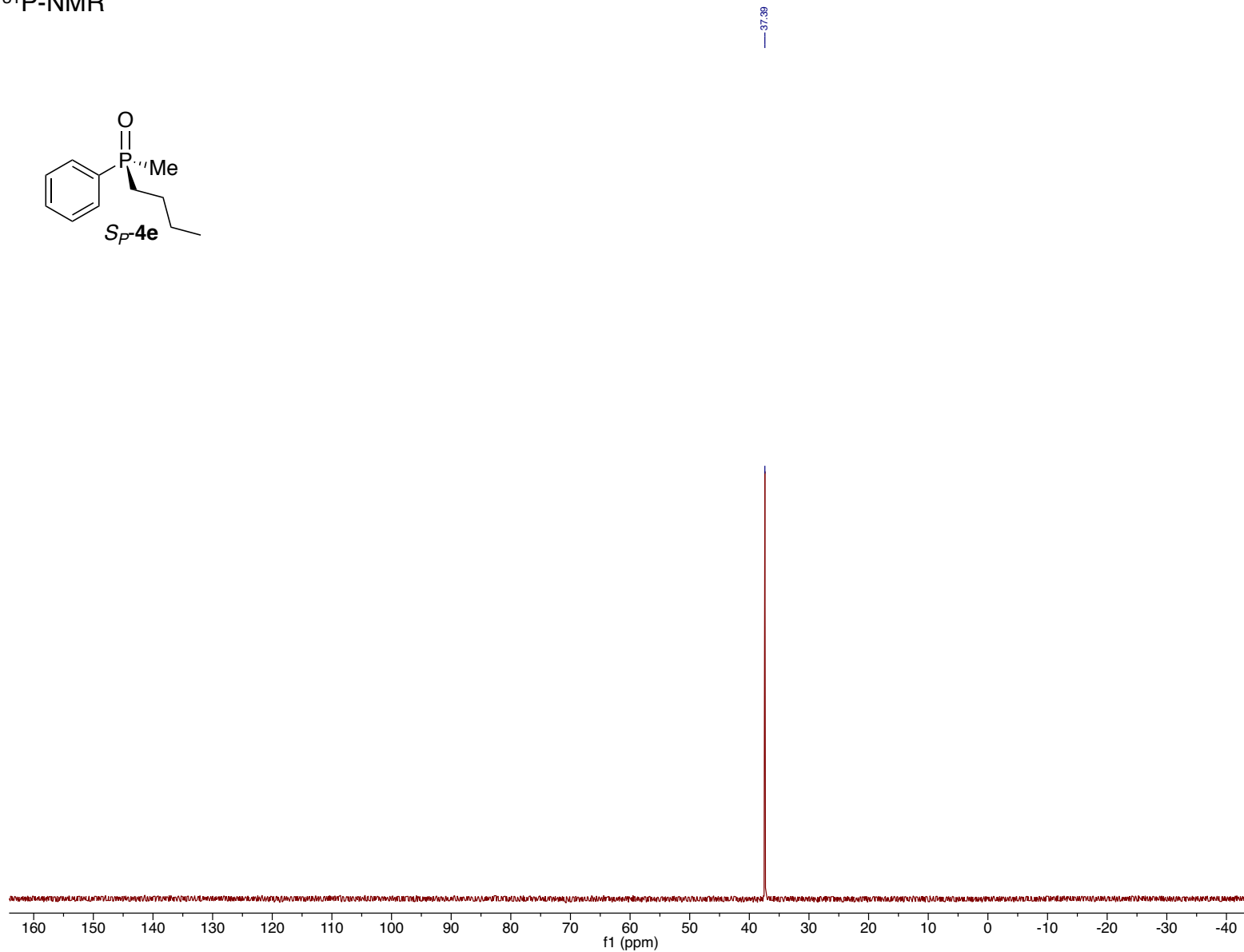
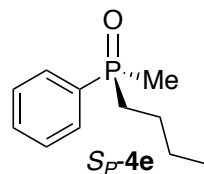
^{31}P -NMR

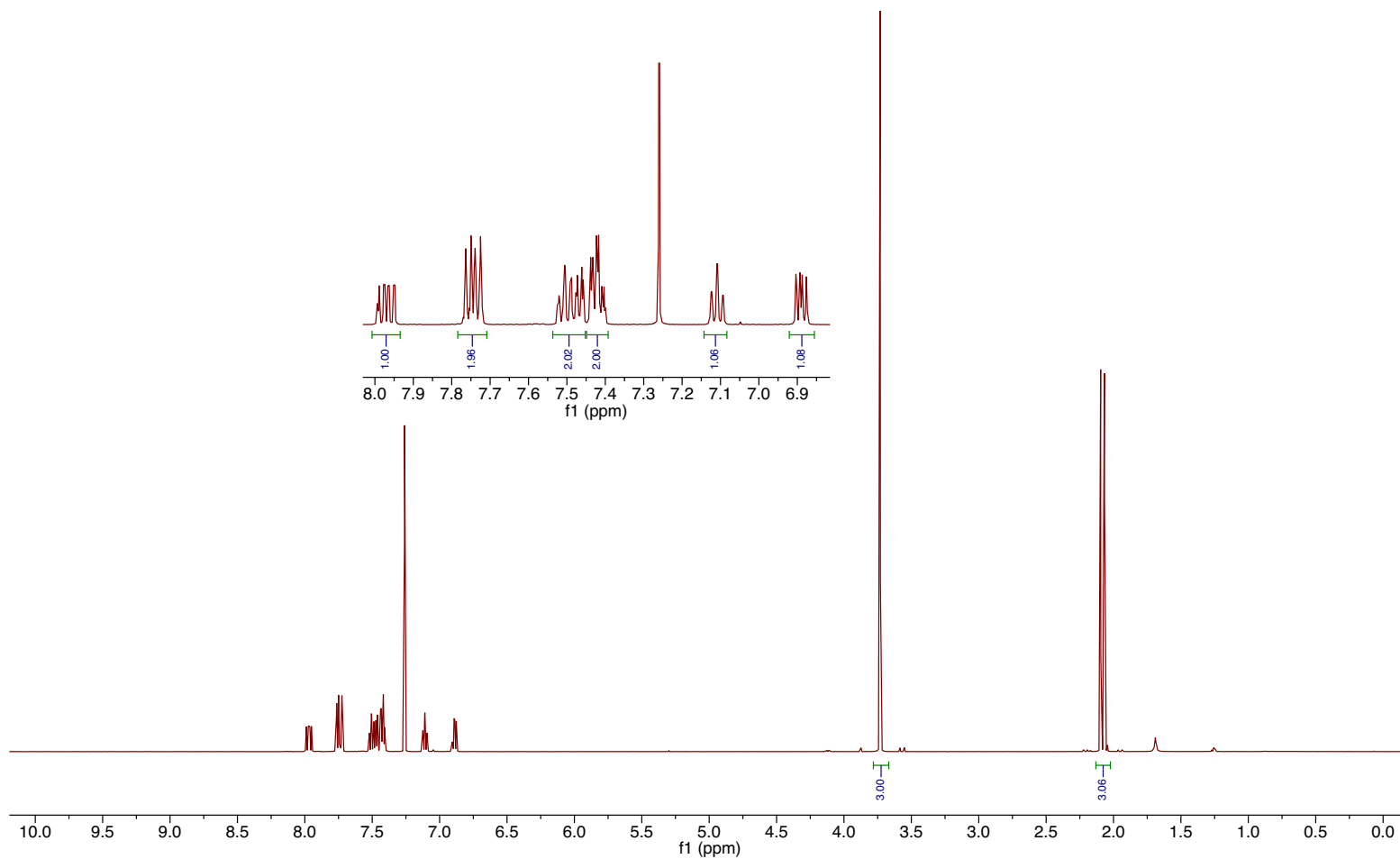
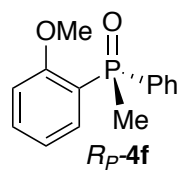


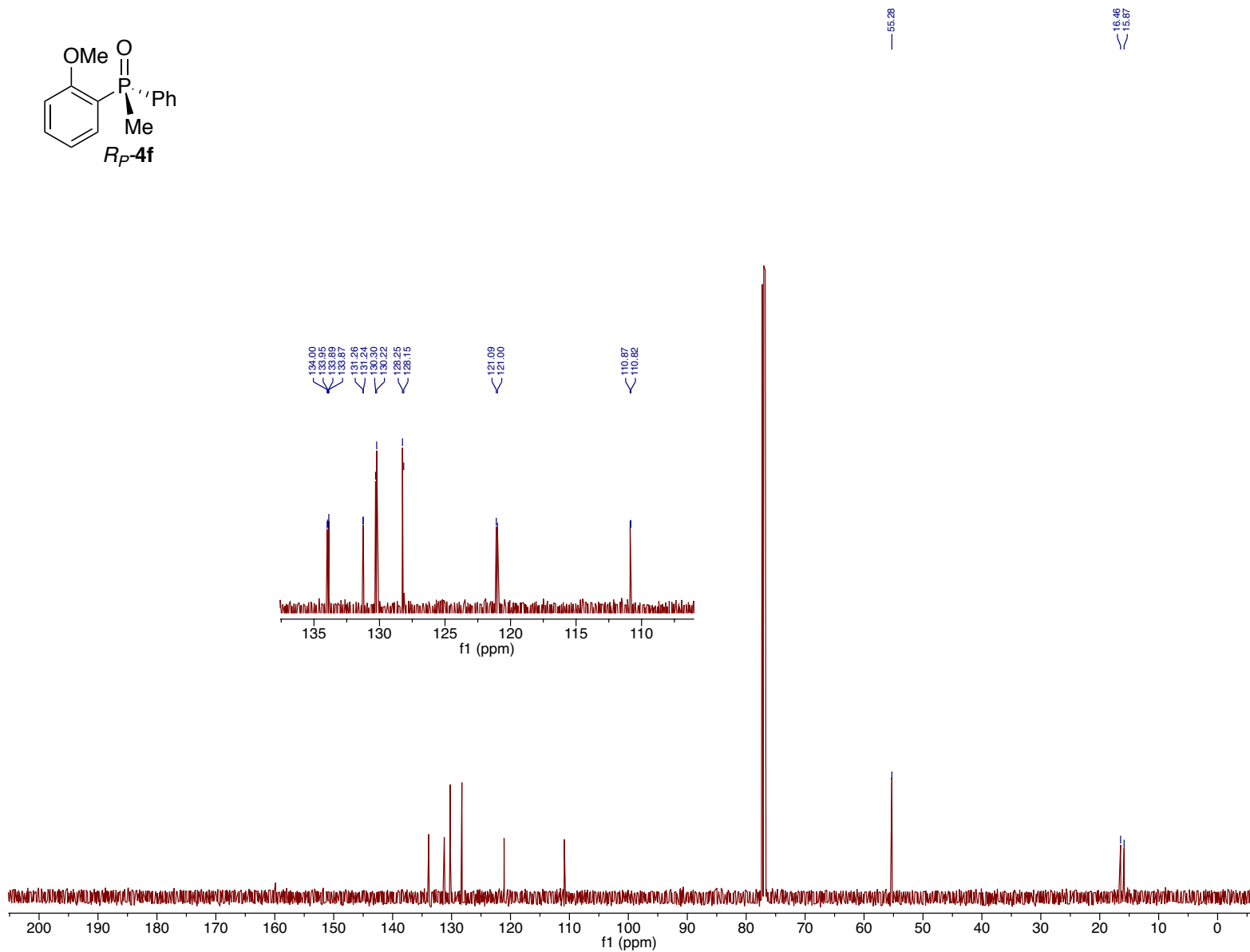
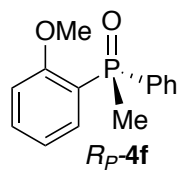




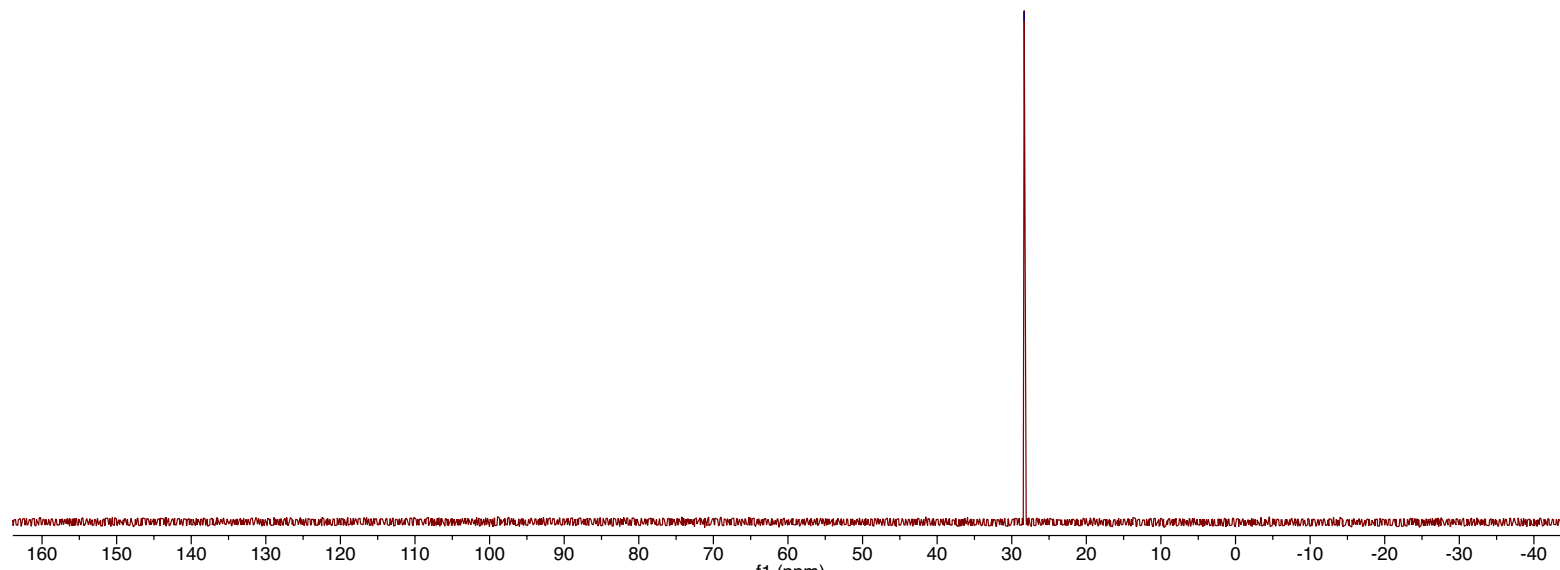
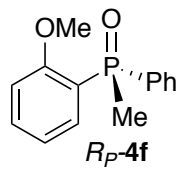
^{31}P -NMR

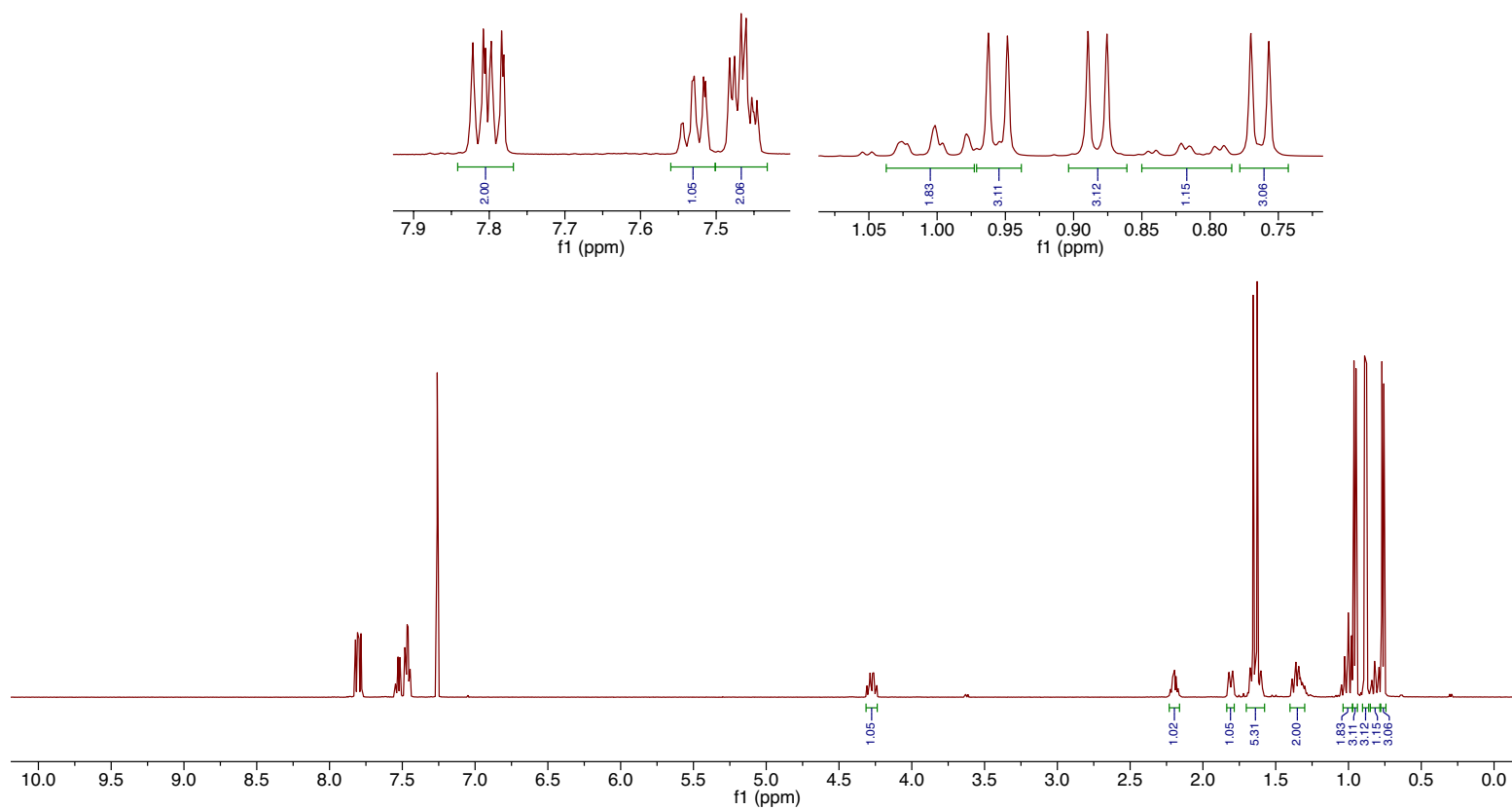
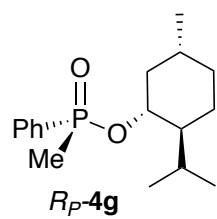


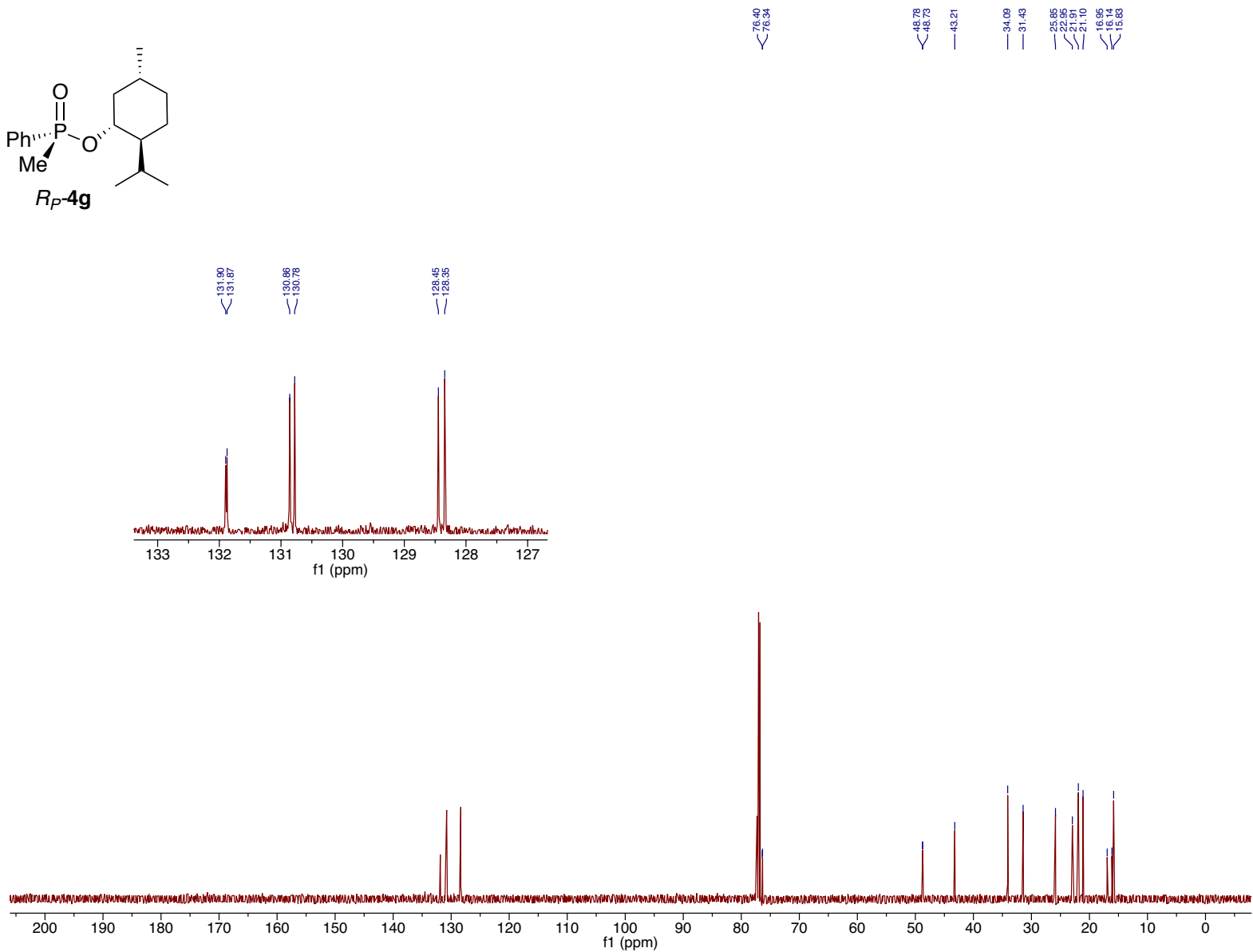
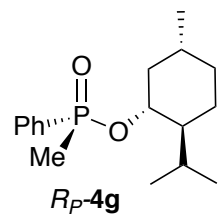




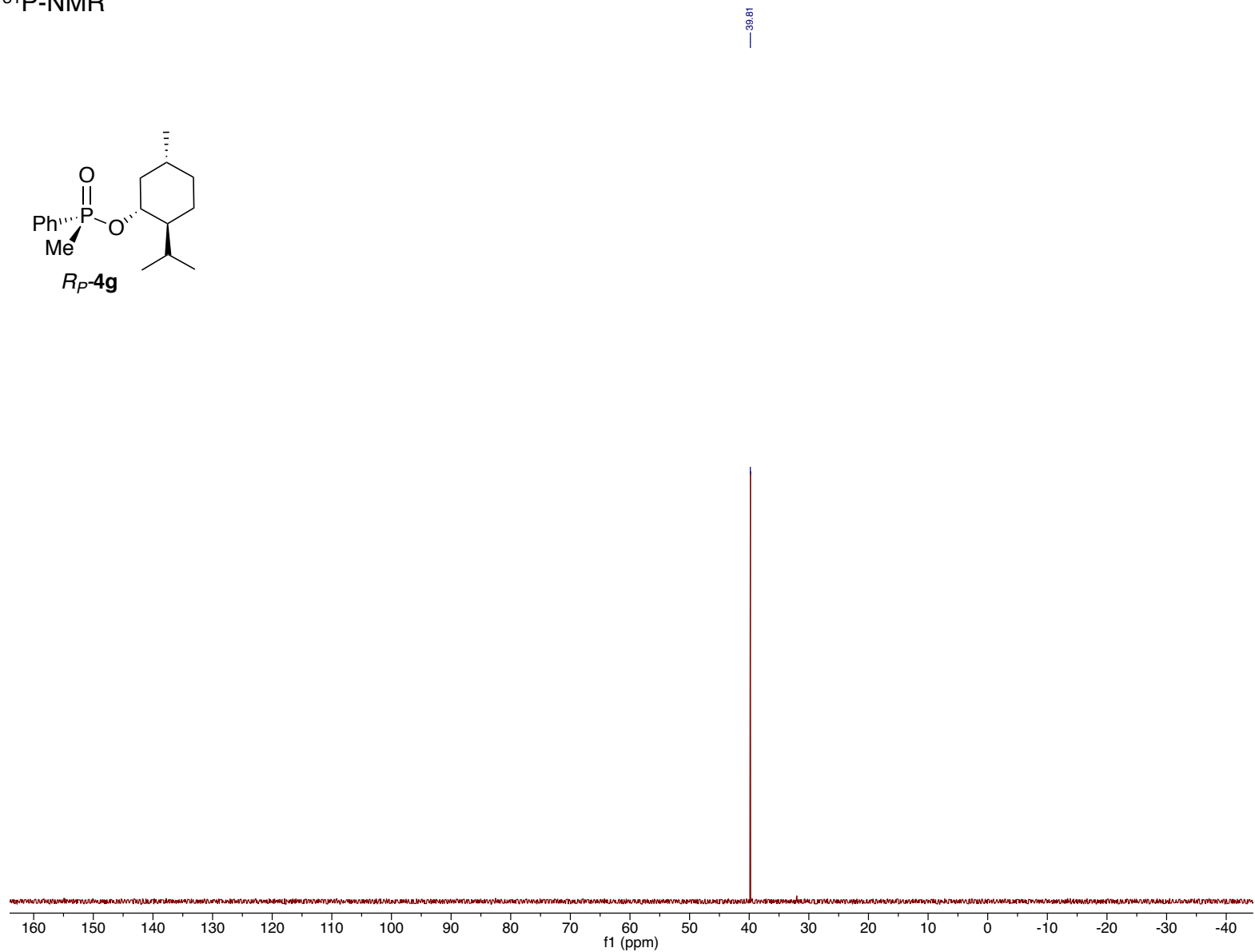
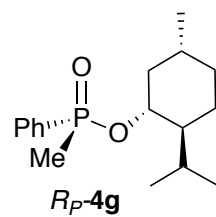
^{31}P -NMR

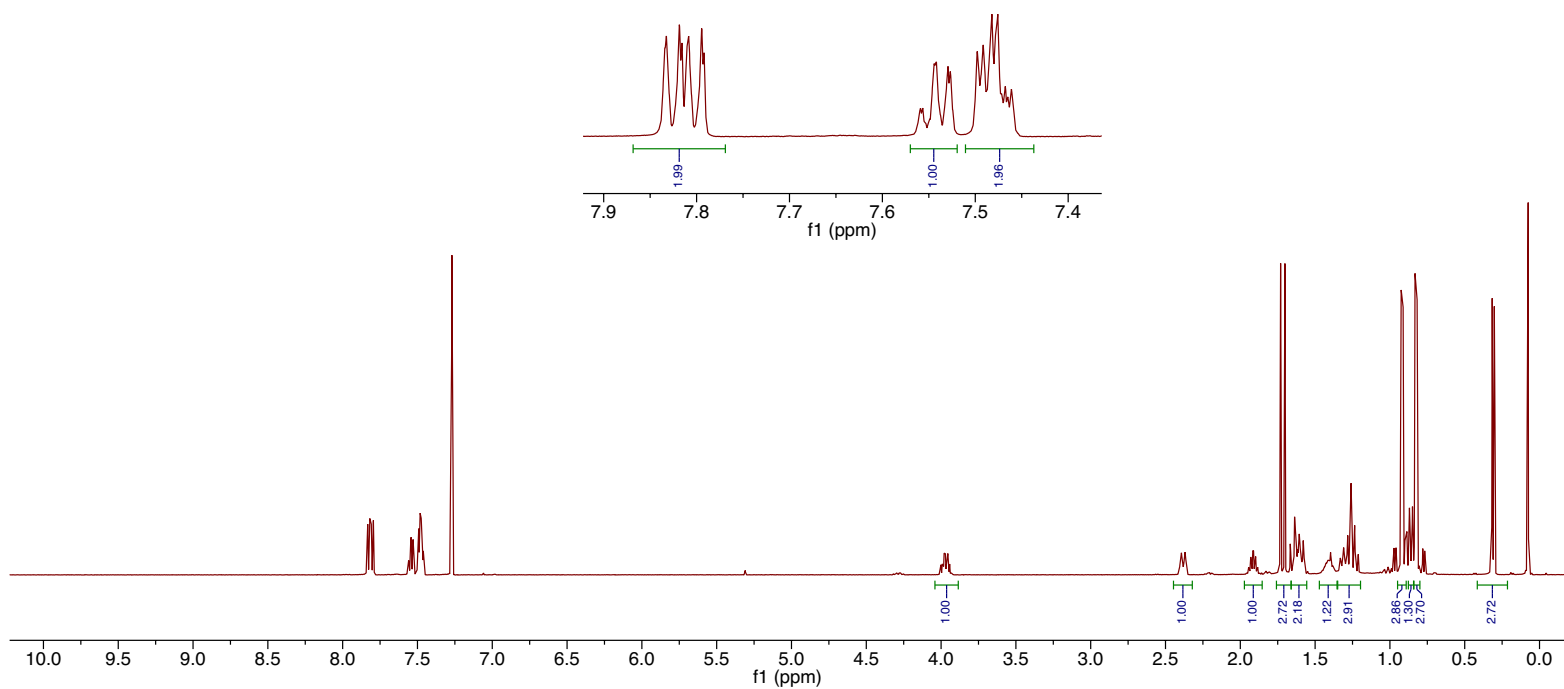
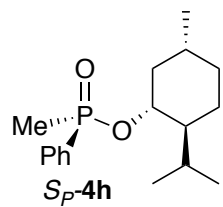


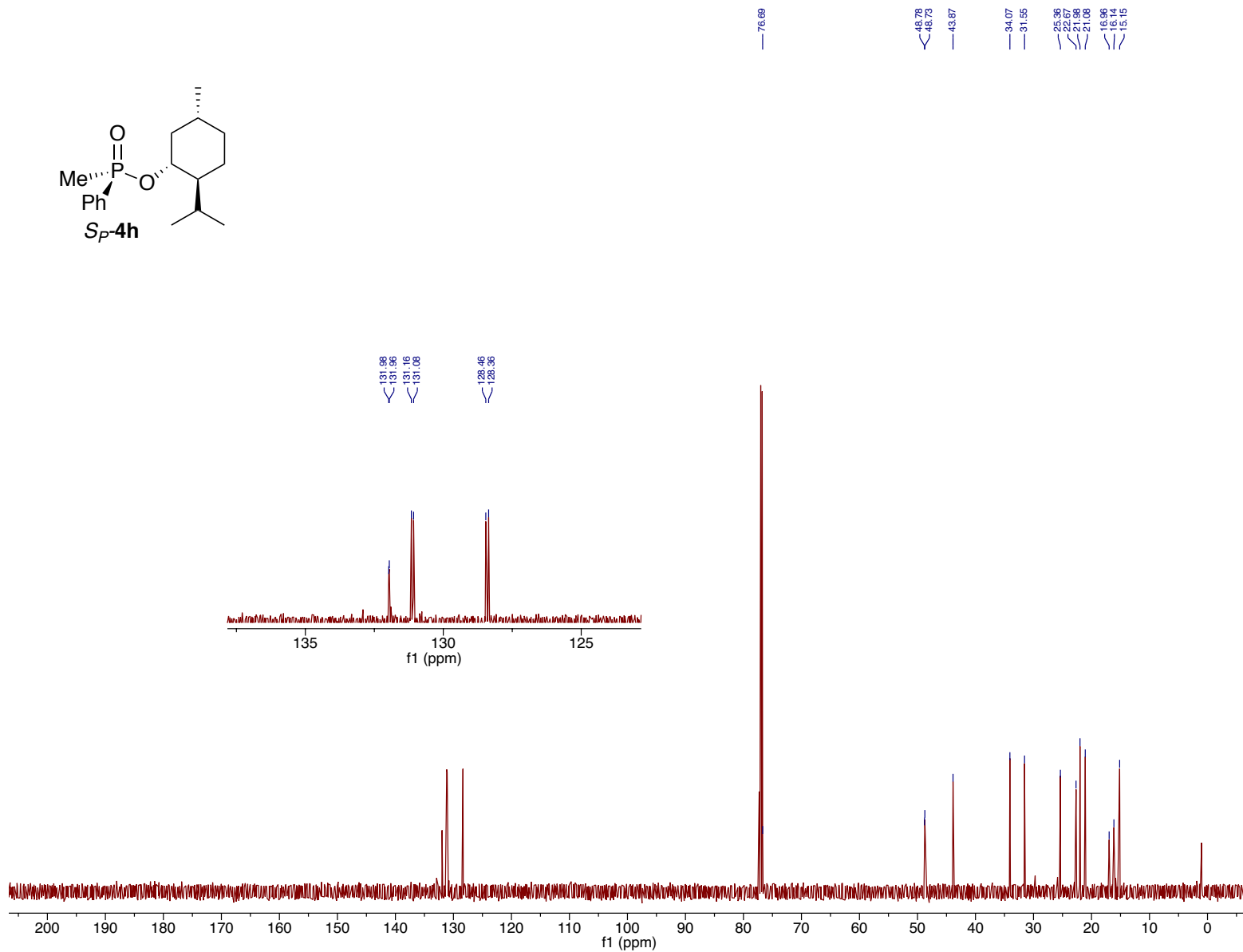
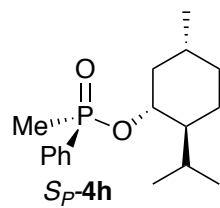




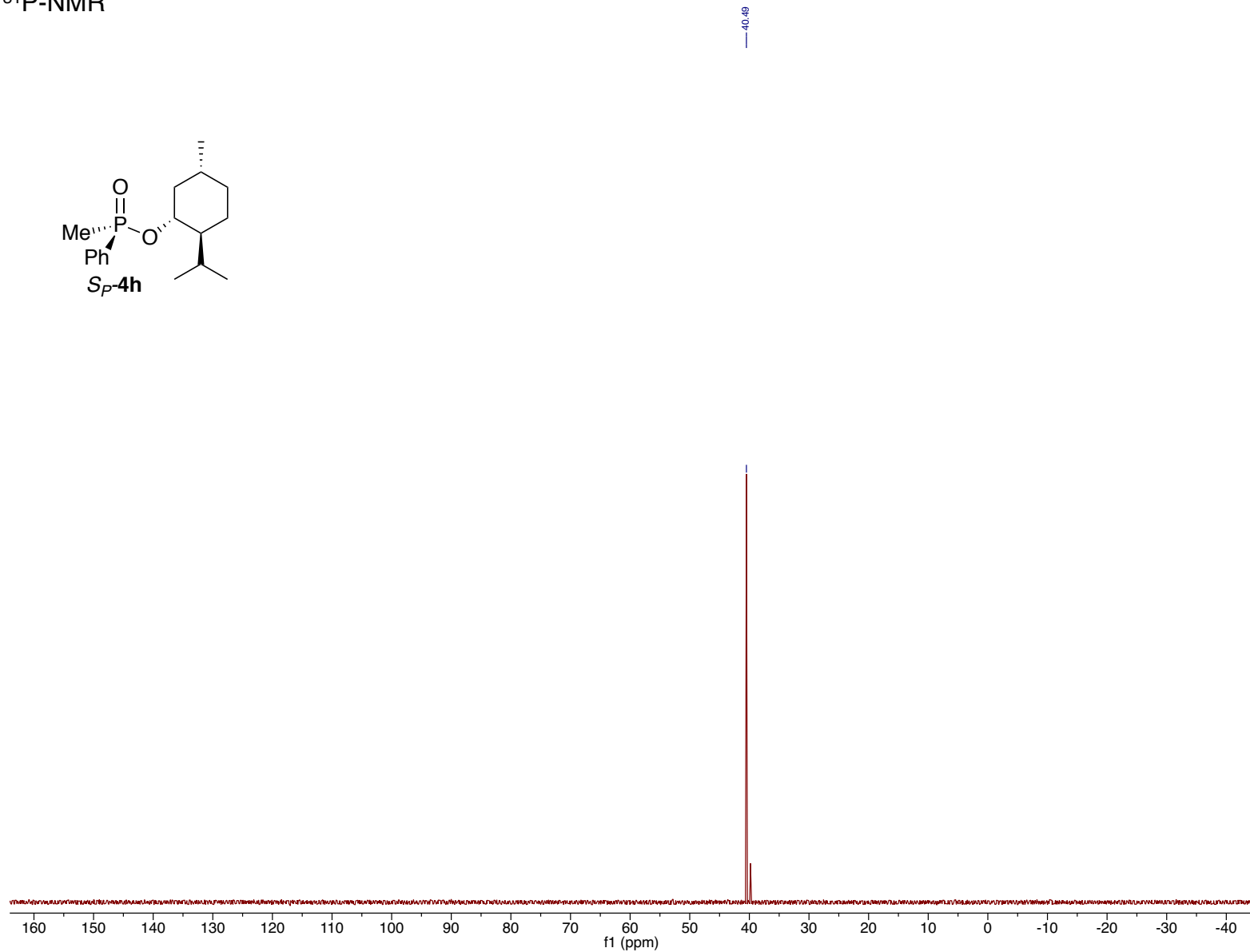
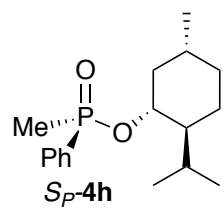
³¹P-NMR

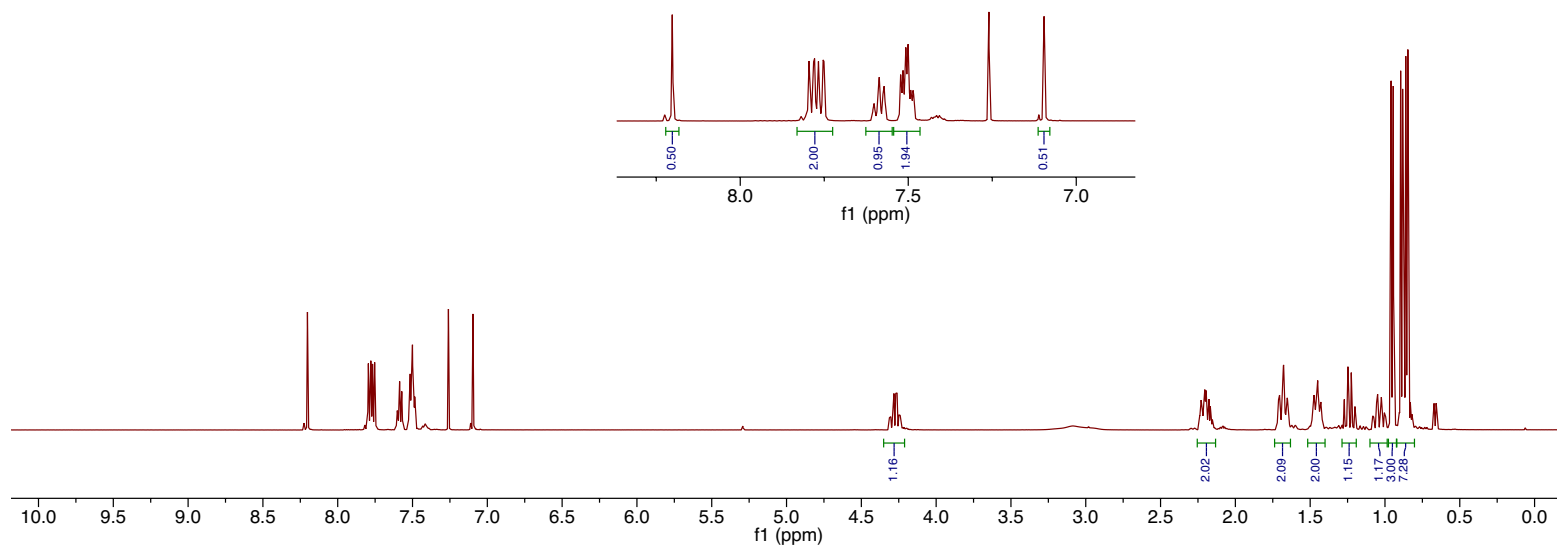
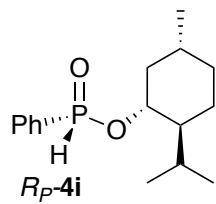


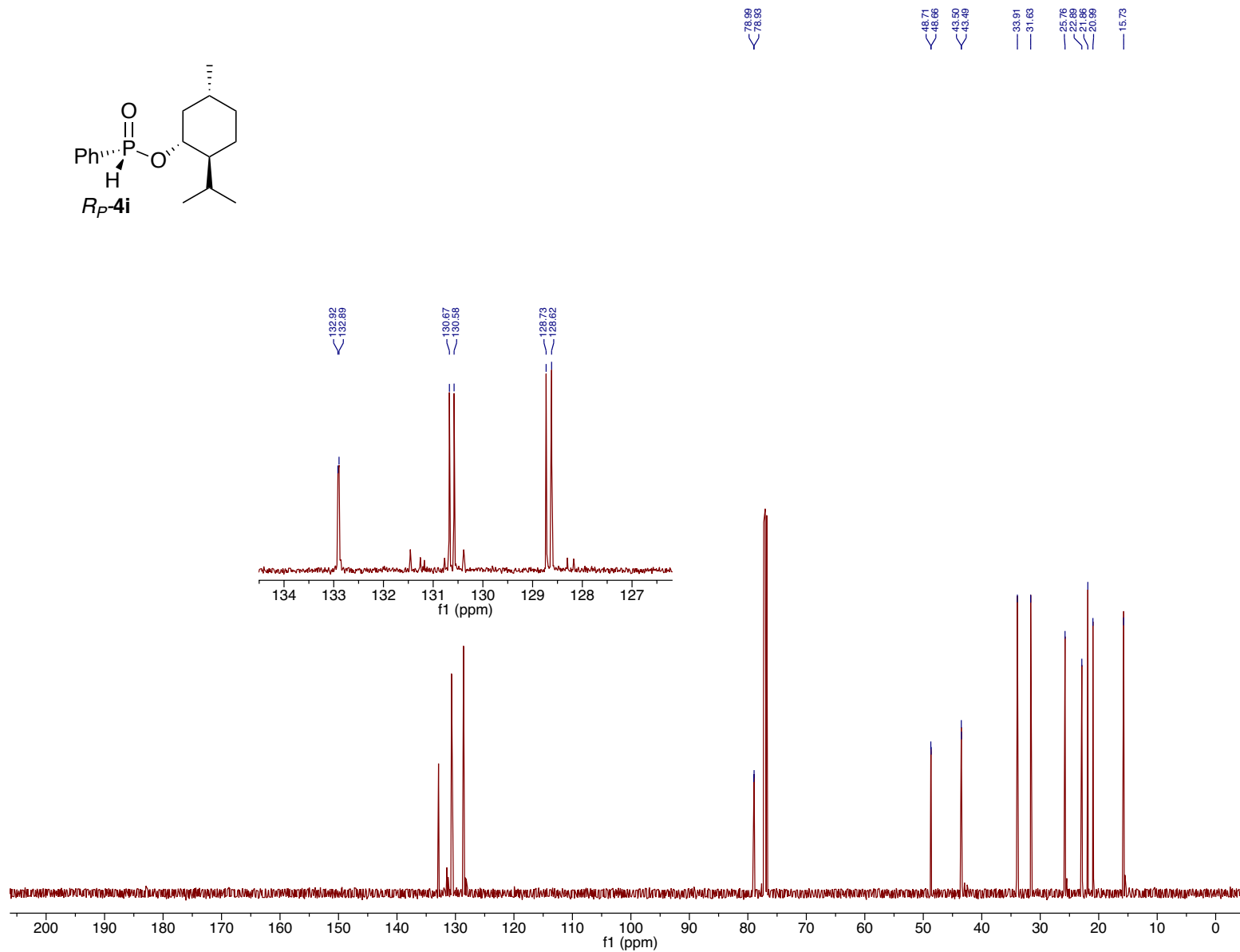
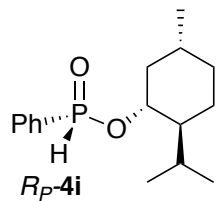




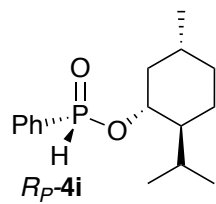
^{31}P -NMR







³¹P-NMR



24.73

